Physica C : Superconductivity **533**, 20-35 (2017)

Type-1.5 superconductivity in multicomponent systems.

E. Babaev[1], J. Carlström[2], M. Silaev[1] and J.M. Speight[3]

[1] *Department of Theoretical Physics and Center for Quantum Materials, The Royal Institute of Technology, Stockholm, SE-10691 Sweden*

[2] *Department of Physics, University of Massachusetts Amherst, MA 01003 USA*

[3] *School of Mathematics, University of Leeds, Leeds LS2 9JT, UK*

arXiv:1608.02211v2 [cond-mat.supr-con] 26 Feb 2017

In general a superconducting state breaks multiple symmetries and, therefore, is characterized by several different coherence lengths ξ_i, $i = 1, ..., N$. Moreover in multiband material even superconducting states that break only a single symmetry are nonetheless described, under certain conditions by multi-component theories with multiple coherence lengths. As a result of that there can appear a state where some coherence lengths are larger and some are smaller than the magnetic field penetration length λ: $\xi_1 \leq \xi_2 ... < \sqrt{2}\lambda < \xi_M \leq ...\xi_N$. That state was recently termed "type-1.5" superconductivity. This breakdown of type-1/type-2 dichotomy is rather generic near a phase transition between superconducting states with different symmetries. The examples include the transitions between $U(1)$ and $U(1) \times U(1)$ states or between $U(1)$ and $U(1) \times Z_2$ states. The later example is realized in systems that feature transition between s-wave and $s + is$ states. The extra fundamental length scales have many physical consequences. In particular in these regimes vortices can attract one another at long range but repel at shorter ranges. Such a system can form vortex clusters in low magnetic fields. The vortex clustering in the type-1.5 regime gives rise to many physical effects, ranging from macroscopic phase separation in domains of different broken symmetries, to unusual transport properties. *Prepared for the proceedings of Vortex IX conference, Rhodes 12-17 September 2015.*

I. INTRODUCTION

Below we briefly discuss the properties and occurrence of "type-1.5" superconducting state characterized by multiple coherence length, some of which are smaller and some larger than the magnetic field penetration length[1] $\xi_1 \leq \xi_2 ... < \sqrt{2}\lambda < \xi_M \leq ...\xi_N$. Type-1 superconductors expel weak magnetic fields, while strong fields give rise to formation of macroscopic phase separation in the form of domains of Meissner and normal states.[2,3] The response of type-2 superconductors is the following:[4] below some critical value H_{c1}, the field is expelled. Above this value a superconductor forms a lattice or a liquid of vortices which carry magnetic flux through the system. Only at a higher second critical value, H_{c2} is superconductivity destroyed. These different responses are

the consequences of the form of the vortex interaction in these systems, the energy cost of a boundary between superconducting and normal states and the thermodynamic stability of vortex excitations. In a type-2 superconductor the energy cost of a boundary between the normal and the superconducting state is negative, while the interaction between vortices is repulsive.[4] This leads to a formation of stable vortex lattices and liquids. In type-1 superconductors the situation is the opposite; the vortex interaction is attractive (thus making them unstable against collapse into one large "giant" vortex), while the boundary energy between normal and superconducting states is positive. The 'ordinary' Ginzburg-Landau model has a critical regime where vortices do not interact.[5,6] The critical value of κ in the most common GL model parameterization corresponds to $\kappa = 1/\sqrt{2}$ (often the factor $1/\sqrt{2}$ is absorbed into the definition of coherence length in which case the critical coupling is $\kappa_c = 1$). The noninteracting regime, which is frequently called the "Bogomolnyi limit" is a property of Ginzburg-Landau model where, at $\kappa_c = 1/\sqrt{2}$, the core-core attractive interaction between vortices cancels at all distances the current-current repulsive interaction[5,6] (up to microscopic corrections beyond the standard Ginzburg-Landau theory). By contrast in multi-component theories are characterized by multiple coherence length and do not in general allow to form a single Ginzburg-Landau parameter κ.

The Ginzburg-Landau free energy functional for a multicomponent superconductor has the form

$$F = \frac{1}{2}\sum_i (D\psi_i)(D\psi_i)^* + V(|\psi_i|) + \frac{1}{2}(\nabla \times \mathbf{A})^2, \tag{1}$$

where ψ_i are complex superconducting components, $D = \nabla + ie\mathbf{A}$, and $\psi_i = |\psi_i|e^{i\theta_i}$, $a = 1, 2$, and $V(|\psi_i|)$ stands for effective potential. We consider a general form of potential terms but the simplest gradient terms. In general Eq.(1) indeed can contain mixed (with respect to components ψ_i) gradient terms, e.g. $Re[D_{\alpha=x,y,z}\psi_i D_{\beta=x,y,z}\psi_j]$ (for a more detail on the effects of these terms see[7]).

The multiple superconducting components can have various origins. First of all they can arise in *(i) superconducting states which break multiple symmetries.* Such systems are described by several order parameters in the sense of Landau theory of phase transitions, and have different coherence lengths associated with them. Multiple broken symmetries are present even in the simplest generalisation of the s-wave superconducting states: the $s + is$ superconducting state,[8,9] which breaks $U(1) \times Z_2$ symmetry.[10] Likewise multiple broken symmetries are present in non-s wave superconductors. Another example is mixtures of independently conserved condensates such as the models for the theoretically discussed superconductivity in metallic hydrogen and hydrogen

rich alloys.[11,12] There ψ_i represents electronic and protonic Cooper pairs or deuteronic condensates. A similar situation was discussed in certain models of nuclear superconductors in the interior of neutron stars, where ψ_i represent protonic and Σ^- hyperonic condensates.[13,14]

Another class of multi-component superconductors is *(ii) systems which are described by multi-component Ginzburg-Landau field theories that do not originate in multiple broken symmetries.* The most common examples are multiband superconductors.[15–17] In this case ψ_i represent superconducting components belonging to different bands. Since a priory there are no symmetry constraints preventing interband Cooper pair tunnelling the theory contains generic terms which describe intercomponent Josephson coupling $\frac{\eta}{2}(\psi_i\psi_j^* + \psi_i\psi_j^*)$. These terms explicitly break symmetry. Here the number of components ψ_i is not dictated by the broken symmetry pattern. Multicomponent GL expansions can be justified when for example $SU(N)$ or $[U(1)]^N$ symmetry is softly explicitly broken down to $U(1)$.[18] Some generalizations of type-1.5 concepts for the case of p-wave pairing in multiband systems was discussed in.[19] Recently rigorous mathematical work was done on justification of multicomponent Ginzburg-Landau expansions.[20]

A. Type-1.5 superconductivity

Multicomponent systems allow a type of superconductivity that is distinct from the type-1 and type-2.[1,7,10,18,21–25] It emerges from the following circumstances: Multi-component GL models have several fundamental scales, namely the magnetic field penetration depth λ and multiple coherence lengths (characteristic scales of the variations of the density fields) ξ_i, which renders the model impossible to parametrize in terms of a single dimensionless parameter κ, thus making the type-1/type-2 dichotomy insufficient for classifying and describing these systems. Rather, in a wide range of parameters, there is a separate superconducting regime with some coherence lengths that are larger and some that are smaller than the magnetic field penetration length $\xi_1/\sqrt{2} < \xi_2/\sqrt{2} < ... < \lambda < \xi_M/\sqrt{2} < ... < \xi_N/\sqrt{2}$. In that regime a situation is possible where vortices have long-range attractive (due to "outer cores" overlap) and short-range repulsive interaction (driven by current-current and electromagnetic interaction) and form vortex clusters coexisting with domains of two-component Meissner state.[1] The first experimental works[24,25] put forward that this state is realized in the two-band material MgB_2. Moshchalkov et al termed this regime "type-1.5 superconductivity".[24] Recently experimental works proposed that this state is realised in Sr_2RuO_4[26,27] and $LaPt_3Si$.[28,29] The experiments on the MgB_2 were done using Bitter decoration, scanning SQUID and scanning Hall probes.[24,25] The analysis of the nature of vortex clustering was

done by cycling field and observing vortex cluster formation in different parts of the sample. In the case of Sr_2RuO_4 the evidence of intrinsic mechanism of vortex cluster formation comes from μSR experiment that observed vortex clusters contraction with decreasing temperature well below T_c thus signaling attractive inter vortex forces rather than pinning responsible for clusterization. The attractive inter vortex forces also provides and explanation for earlier experiment on Sr_2RuO_4[30] that reported vanishing creep in the absence of dramatic increase of critical current [initially in[30] this was attributed to effects of domain walls trapping vortices. However such configurations would have very characteristic magnetic signatures,[31,32] these signatures were not observed in surface probes[26]]. A prediction of a (narrow) region of type-1.5 state was made for certain interface superconductors.[33] Also it was pointed out that a generic type-1.5 regime should form in iron-based superconductors near transitions from s to $s+is$ pairing states.[10] Type-1.5 superconductivity was discussed in the context of the quantum Hall effect[34] and neutron stars.[35] For other recent works on this and related subjects see e.g..[19,36–45]

In these systems one cannot straightforwardly use the usual one-dimensional argument concerning the energy of superconductor-to-normal state boundary to classify the magnetic response. First of all, the energy per vortex in such a case depends on whether a vortex is placed in a cluster or not. Formation of a single isolated vortex might be energetically unfavorable, while formation of vortex clusters can be favorable, because in a cluster (where vortices are placed in a minimum of the interaction potential), the energy per flux quantum is smaller than that for an isolated vortex. Besides the energy of a vortex in a cluster, there appears an additional characteristic associated with the energy of the boundary of a cluster. In other words for systems with inhomogeneous vortex states there are many different interfaces, some of which have positive and some negative free energy. The non-monotonic intervortex interaction is one of key properties of a type-1.5 superconductor, but is not a state-defining one. As discussed in the introduction and also below, intervortex attraction can arise under certain circumstances in single-component materials as well. In type-1.5 case this is a consequence of multiple coherence lengths and comes with a number of new physical effects discussed below. We summarise the basic properties of type-1, type-2 and type-1.5 regimes in the table I .

	single-component type-1	**single-component type-2**	**multi-component Type-1.5**
Characteristic lengths scales	Penetration length λ & coherence length ξ ($\frac{\lambda}{\xi} < \frac{1}{\sqrt{2}}$)	Penetration length λ & coherence length ξ ($\frac{\lambda}{\xi} > \frac{1}{\sqrt{2}}$)	Multiple characteristic density variations length scales ξ_i, and penetration length λ, the non-monotonic vortex interaction occurs in these systems in a large range of parameters when $\xi_1 \leq \xi_2 \leq .... < \sqrt{2}\lambda < \xi_M \leq ... \leq \xi_N$
Intervortex interaction	Attractive	Repulsive	Attractive at long range and repulsive at short range
Energy of superconducting/normal state boundary	Positive	Negative	Under quite general conditions negative energy of superconductor/normal interface inside a vortex cluster but positive energy of the vortex cluster's boundary
The magnetic field required to form a vortex	Larger than the thermodynamical critical magnetic field	Smaller than thermodynamical critical magnetic field	In different cases either (i) smaller than the thermodynamical critical magnetic field or (ii) larger than critical magnetic field for single vortex but smaller than critical magnetic field for a vortex cluster of a certain critical size
Phases in external magnetic field	(i) Meissner state at low fields; (ii) Macroscopically large normal domains at elevated fields. First order phase transition between superconducting (Meissner) and normal states	(i) Meissner state at low fields, (ii) vortex lattices/liquids at larger fields. Second order phase transitions between Meissner and vortex states and between vortex and normal states at the level of mean-field theory.	(i) Meissner state at low fields (ii) Macroscopic phase separation into vortex clusters coexisting with Meissner domains at intermediate fields (iii) Vortex lattices/liquids at larger fields. Vortices form via a first order phase transition. The transition from vortex states to normal state is second order.
Energy E(N) of N-quantum axially symmetric vortex solutions	$\frac{E(N)}{N} < \frac{E(N-1)}{N-1}$ for all N. Vortices collapse onto a single N-quantum mega-vortex	$\frac{E(N)}{N} > \frac{E(N-1)}{N-1}$ for all N. N-quantum vortex decays into N infinitely separated single-quantum vortices	There is a characteristic number N_c such that $\frac{E(N)}{N} < \frac{E(N-1)}{N-1}$ for $N < N_c$, while $\frac{E(N)}{N} > \frac{E(N-1)}{N-1}$ for $N > N_c$. N-quantum vortices decay into vortex clusters.

TABLE I. Basic characteristics of bulk clean superconductors in type-1, type-2 and type-1.5 regimes. Here the most common units are used in which the value of the GL parameter which separates type-1 and type-2 regimes in a single-component theory is $\kappa_c = 1/\sqrt{2}$. Magnetization curves in these regimes are shown on Fig. 1

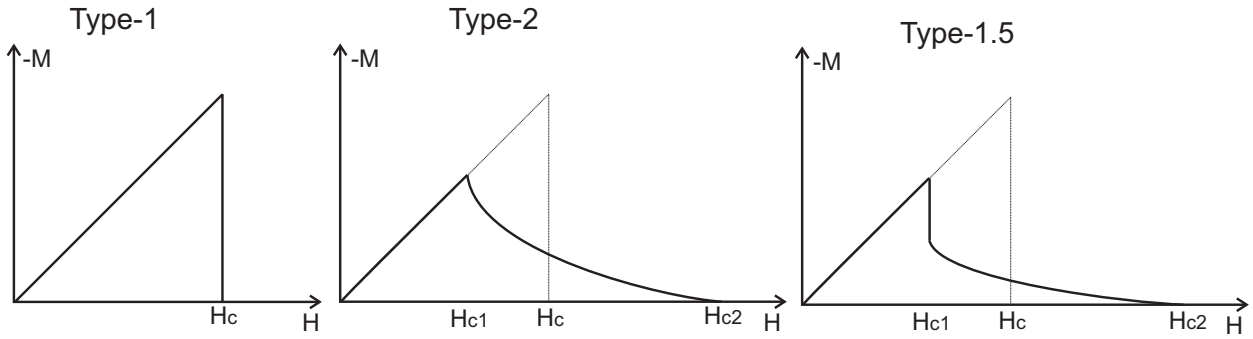

FIG. 1. A schematic picture of magnetization curves of type-1, type-2 and type-1.5 superconductors. The magnetisation jump at H_{c1} is one of the features of type-1.5 regime, however it is not a state-defining property conversion of the H_{c1} phase transition to a first order one can be caused by a number of reasons (e.g. microscopic corrections near Bogomolnyi point, multi-layer structure, etc) in ordinary type-2 superconductors

II. THE TWO-BAND GINZBURG-LANDAU MODEL WITH ARBITRARY INTERBAND INTERACTIONS. DEFINITION OF THE COHERENCE LENGTHS AND TYPE-1.5 REGIME

A. Free energy functional

Realization of the type-1.5 regime requires at least two superconducting components. In this section we study the type-1.5 regime using the following two-component Ginzburg-Landau (TCGL) free energy functional.

$$F = \frac{1}{2}(D\psi_1)(D\psi_1)^* + \frac{1}{2}(D\psi_2)(D\psi_2)^* - \nu Re\Big\{(D\psi_1)(D\psi_2)^*\Big\} + \frac{1}{2}(\nabla\times\mathbf{A})^2 + F_p \qquad (2)$$

Here $D = \nabla + ie\mathbf{A}$, and $\psi_i = |\psi_i|e^{i\theta_i}$, $i = 1, 2$, represent two superconducting components. While in general two components can have different critical temperatures, in the simplest case, the two-band superconductor breaks only $U(1)$ symmetry. Then eq. (2) can be obtained as an expansion of the free energy in small gaps and small gradients.[17,18,46–49] Such an expansion should not be confused with the simplest expansion in a single small parameter $\tau = (1 - T/T_c)$. The τ-based expansion for $U(1)$ system is an approximation that yields only one order parameter for a $U(1)$ system and neglects the second coherence length. The multi-parameter expansions that are not based on symmetry are justified under certain conditions.[18,49] Indeed the existence of two bands in a superconductor by itself is not a sufficient conditions for a superconductor to be described by a model like (2) with two well-defined coherence lengths. For discussion of the applicability conditions

of the theory (2) for two-band $U(1)$ systems see.[18,22] Note that, in general in two-band expansion, the terms corresponding to one component can be larger than a terms contributed by another component. However as it will be clear below, for the discussion of typology of superconductors, the relevant parameters are characteristic length scales associated with the exponential laws at which field component restore their ground state values away from a perturbation such as a vortex core (i.e. the coherence lengths). Indeed a component with *smaller amplitude* can give raise to a *longer coherence length* that is important for intervortex interaction and should not be discarded based merely on the smallness of amplitude $|\psi_i|$. In principle, for the component with larger amplitude, one can keep higher-power terms in the GL expansion such as $\psi_i\psi_i^*(D\psi_i)(D\psi_i)^*, |\psi_i|^6$ etc. These terms lead to some corrections to two coherence lengths, while not affecting the overall form of intervortex forces as can be seen from the analysis in.[7] As be seen from the comparison of vortex solutions in the GL formalism and in microscopic model without GL expansion,[18] in the regime of most interest these terms can be neglected.

We begin with the most general analysis by considering the case where F_p can contain an *arbitrary* collection of non-gradient terms, of arbitrary power in ψ_i representing various inter and intra-band interactions. Below we show how three characteristic length scales are defined in this two component model (two associated with density variations and the London magnetic field penetration length).

The only vortex solutions of the model (2) which have finite energy per unit length are the integer N-flux quantum vortices which have the following phase windings along a contour l around the vortex core: $\oint_l \nabla\theta_1 = 2\pi N, \oint_l \nabla\theta_2 = 2\pi N$ which can be denoted as (N,N). Vortices with differing phase windings (N,M) carry a fractional multiple of the magnetic flux quantum and have energy divergent with the system size,[50] which under usual conditions makes them irrelevant for the physics of magnetic response of a bulk system.

In what follows we investigate only the integer flux vortex solutions which are the energetically cheapest objects to produce by means of an external field in a bulk superconductor. Note that since this object is essentially a bound state of two vortices, it in general will have two different co-centered cores.

III. COHERENCE LENGTHS AND INTERVORTEX FORCES AT LONG RANGE IN MULTI-BAND SUPERCONDUCTORS

In this section we give criterion for attractive or repulsive force between well separated vortices in system (2) and condition for non-monotonic inter vortex forces following.[1,7,21] We show how it can be determined by analyzing F_p when $\nu = 0$ and how three fundamental length scales are defined in the model (2). If the model has mixed gradient terms they can be either treated as in Ref.[7] or eliminated by a linear transformation. By gauge invariance, F_p may depend only on $|\psi_1|$, $|\psi_2|$ and $\delta = \theta_1 - \theta_2$. We consider the regime when F_p has a global minimum at some point other than the one with $|\psi_i| = 0$, namely at $(|\psi_1|, |\psi_2|, \delta) = (u_1, u_2, 0)$ where $u_1 > 0$ and $u_2 \geq 0$ (for discussion of phase-separated regimes see[43]). Then the model has a trivial solution, $\psi_1 = u_1$, $\psi_2 = u_2$, $A = 0$, (i.e. the ground state). Here we are interested in models that support axially-symmetric single-vortex solutions of the form

$$\psi_i = f_i(r)e^{i\theta}\,, \qquad\qquad (A_1, A_2) = \frac{a(r)}{r}(-\sin\theta, \cos\theta) \tag{3}$$

where f_1, f_2, a are real profile functions with boundary behavior $f_i(0) = a(0) = 0$, $f_i(\infty) = u_i$, $a(\infty) = -1/e$. No explicit expressions for f_i, a are known, but, by analyzing the system of differential equations they satisfy, one can construct asymptotic expansions for them at large r, see.[7,21]

At large r from the vortex in the model (2) the system recovers (up to exponentially small corrections) the ground state. In fact, the long-range field behavior of a vortex solution can be identified with a solution of the linearization of the model about the ground state, in the presence of appropriate point sources at the vortex positions. This idea is explained in detail for single component GL theory in.[51] A common feature of topological solitons (vortices being a particular example) is that the forces they exert on one another coincide asymptotically (at large separation) with those between the corresponding point-like perturbations (point sources) interacting via the linearized field theory.[52] For (2), the linearization has one vector (A) and 3 real scalar ($\epsilon_1 = |\psi_1| - u_1$, $\epsilon_2 = |\psi_2| - u_2$ and δ) degrees of freedom. The isolated vortex solutions have, by definition within the ansatz we use, $\delta \equiv 0$ everywhere. Hence have no source for δ, so we can set $\delta = 0$ in the linearization, which becomes

$$F_{lin} = \frac{1}{2}|\nabla\epsilon_1|^2 + \frac{1}{2}|\nabla\epsilon_2|^2 + \frac{1}{2}\begin{pmatrix}\epsilon_1\\ \epsilon_2\end{pmatrix}\cdot\mathcal{H}\begin{pmatrix}\epsilon_1\\ \epsilon_2\end{pmatrix} + \frac{1}{2}(\partial_1 A_2 - \partial_2 A_1)^2 + \frac{1}{2}e^2(u_1^2 + u_2^2)|A|^2. \tag{4}$$

Here, $\mathcal{H}$ is the Hessian matrix of $F_p(|\psi_1|, |\psi_2|, 0)$ about (u_1, u_2), that is,

$$\mathcal{H}_{ij} = \left.\frac{\partial^2 F_p}{\partial|\psi_i|\partial|\psi_j|}\right|_{(u_1,u_2,0)}. \tag{5}$$

Note that, in F_{lin}, the vector potential field A decouples from the scalar fields ψ_i. This mode mediates a repulsive force between vortices (originating in current-current and magnetic interaction) with decay length which is the London's magnetic field penetration length $\lambda = 1/\mu_A$ where μ_A is the mass of the field, that is,

$$\mu_A = e\sqrt{u_1^2 + u_2^2}. \tag{6}$$

By contrast, the scalar fields ϵ_1, ϵ_2 are, in general, coupled (i.e. the symmetric matrix $\mathcal{H}$ has off-diagonal terms). To remove the cross-terms one should find a proper linear combination of the fields that correspond to normal modes of the system. To this end we make a linear redefinition of fields, expanding $(\epsilon_1, \epsilon_2)^T$ with respect to the orthonormal basis for $\mathbb{R}^2$ formed by the eigenvectors v_1, v_2 of $\mathcal{H}$,

$$(\epsilon_1, \epsilon_2)^T = \chi_1 v_1 + \chi_2 v_2. \tag{7}$$

The corresponding eigenvalues μ_1^2, μ_2^2 are necessarily real (since $\mathcal{H}$ is symmetric) and positive (since (u_1, u_2) is a minimum of F_p), and hence

$$F_{lin} = \frac{1}{2}\sum_{a=1}^{2}\left(|\nabla\chi_i|^2 + \mu_i^2\chi_i^2\right) + \frac{1}{2}(\partial_1 A_2 - \partial_2 A_1)^2 + \frac{1}{2}e(u_1^2 + u_2^2)|A|^2. \tag{8}$$

The scalar fields χ_1, χ_2 describe linear combination of the original density fields. The new fields recover ground state values at different characteristic length scales. The characteristic length scales are nothing but coherence lengths which are given by inverse of μ_i

$$\xi_1 \equiv 1/\mu_1\,, \qquad\qquad \xi_2 \equiv 1/\mu_2 \tag{9}$$

respectively *(here and below we absorb the factor $1/\sqrt{2}$ in the definition of coherence length)*. Each of these field defines a vortex core of some characteristic size that mediate an attractive force between vortices at long range. In terms of the normal-mode fields χ_1, χ_2 and A, the composite point source which must be introduced into F_{lin} to produce field configurations identical to those of vortex asymptotics is

$$\kappa_1 = q_1\delta(x)\,, \qquad \kappa_2 = q_2\delta(x)\,, \qquad \mathbf{j} = m(\partial_2, -\partial_1)\delta(x)\,, \tag{10}$$

where κ_1 is the source for χ_1, κ_2 the source of χ_2, $\mathbf{j}$ the source for $\mathbf{A}$, $\delta(x)$ denotes the two dimensional Dirac delta function and q_1, q_2 and m are unknown real constants which can, in principle, be determined numerically by a careful analysis of the vortex asymptotics. Physically, a vortex, as seen from a long distance can be thought of as a point particle carrying two different types of scalar monopole charge, q_1, q_2, inducing fields of mass μ_1, μ_2 respectively, and a magnetic dipole moment m oriented orthogonal to the x_1x_2 plane, inducing a massive vector field of mass $\mu_A \equiv \lambda^{-1}$. The interaction energy experienced by a pair of point particles carrying these sources, held distance r apart, is easily computed in linear field theory. For example, two scalar monopoles of charge q inducing fields of mass μ held at positions $\mathbf{y}$ and $\tilde{\mathbf{y}}$ in $\mathbb{R}^2$ experience interaction energy

$$E_{int} = -\int_{\mathbb{R}^2} \kappa\tilde{\chi} = -\int_{\mathbb{R}^2} q\delta(\mathbf{x}-\mathbf{y})\frac{q}{2\pi}K_0(\mu|\mathbf{y}-\tilde{\mathbf{y}}|) = -\frac{q^2}{2\pi}K_0(\mu|\mathbf{y}-\tilde{\mathbf{y}}|) \tag{11}$$

where κ is the source for the monopole at $\mathbf{y}$, $\tilde{\chi}$ is the scalar field induced by the monopole at $\tilde{\mathbf{y}}$[51] and K_0 denotes the modified Bessel's function of the second kind. The interaction energy for a pair of magnetic dipoles may be computed similarly. In the case of our two component GL model, the total long-range inter-vortex interaction energy has three terms, corresponding to the three sources in the composite point source (10), and turns out to be

$$E_{int} = \frac{m^2}{2\pi}K_0(\mu_A r) - \frac{q_1^2}{2\pi}K_0(\mu_1 r) - \frac{q_2^2}{2\pi}K_0(\mu_2 r). \tag{12}$$

Note that, the first term in this formula which originates in magnetic and current-current interaction is repulsive, while the other two as associated with core-core interactions of two kinds of co-centered cores are attractive. The linearized theory does not contain information about the prefactors q_1, q_2 and m. However they can be determined numerically from the full nonlinear GL theory. At very large r, $E_{int}(r)$ is dominated by whichever term corresponds to the smallest of the three masses, μ_A, μ_1, μ_2, so to determine whether vortices attract at long range, it is enough to compute just these masses. The generalization to the case with larger number of components is straightforward: additional coherence lengths give additional contributions to attractive interaction in the form $-\frac{q_i^2}{2\pi}K_0(\mu_i r)$. Generalizations to multiple repulsive length scales in layered systems or caused by stray fields were discussed in[39] . In thin films intervortex interaction acquires also $1/r$ repulsion at long ranges due to the magnetic field outside the sample, similarly to single-component case.[53]

Consider the case where long-range interaction is attractive due to ξ_1 being the largest length scale of the problem. The criterion for short-range repulsive interaction is thermodynamic stability of vortices which is equivalent to the condition that the system has solution with negative free

energy interfaces in external fields.[1,7,21] Indeed when the interface energy is always positive the system exhibits type-1 behavior: i.e. tends to form a single vortex with high finding number. If there are interfaces with negative energy in the external field, the system tends to maximize these interfaces. In the type-1.5 regime the system forms vortex clusters, where it maximizes number of vortex cores inside the vortex clusters. A the same time the system minimizes the interface of the cluster itself (that costs positive energy).

To summarize, the nature of intervortex forces at large separation in the model under consideration, can be determined purely by analyzing F_p: one finds the ground state (u_1, u_2) and the Hessian $\mathcal{H}$ of F_p about (u_1, u_2). From this one computes the mass of the vector field A, $\mu_A = e\sqrt{u_1^2 + u_2^2}$ (i.e. the inverse of the magnetic field penetration length), and the masses μ_1, μ_2 of the scalar normal modes (i.e. the inverses of the coherence lengths). These masses being the square roots of the eigenvalues of $\mathcal{H}$. If either (or both) of μ_1, μ_2 are less than μ_A, then the dominant interaction at long range is attractive (i.e. vortex core extends beyond the area where magnetic field is localized), while if μ_A is less than both μ_1 and μ_2, the dominant interaction at long range is repulsive. The special feature of the two-component model is that the vortices where core extends beyond the magnetic field penetration length are thermodynamically stable in a range of parameters and moreover one can have a repulsive force between the vortices at shorter distances where the system has thermodynamically stable vortex solutions.[1,7,21] It is important to stress that length scales μ_1^{-1}, μ_2^{-1} are not directly associated with the individual condensates ψ_1, ψ_2. Rather they are associated with the normal modes χ_1, χ_2, defined as[7,21]

$$\chi_1 = (|\psi_1| - u_1)\cos\Theta - (|\psi_2| - u_2)\sin\Theta\,, \quad \chi_2 = -(|\psi_1| - u_1)\sin\Theta - (|\psi_2| - u_2)\cos\Theta\,. \tag{13}$$

These may be thought of as rotated (in field space) versions of $\epsilon_1 = |\psi_1| - u_1$, $\epsilon_2 = |\psi_2| - u_2$. The *mixing angle*, that is, the angle between the χ and ϵ axes, is Θ, where the eigenvector v_1 of $\mathcal{H}$ is $(\cos\Theta, \sin\Theta)^T$. This, again, can be determined directly from $\mathcal{H}$.

Note also that the shorter of the length scales μ_1^{-1}, μ_2^{-1}, although being a fundamental length scale of the theory, can be masked in a density profile of a vortex solution by nonlinear effects. This, for example certainly happens if $\mu_1^{-1} \ll \mu_A \equiv \lambda^{-1}$ (see short discussion in Ref.[21]). Also note that in general the minimum of the interaction potential will not be located at the London penetration length, because it in general will be also affected by nonlinearities.

From the discussion above it follows that in general one cannot drop the subdominant component based on comparison of the ground state values of the amplitudes of $|\psi_i|$ in the GL expansion. Namely, the long-range interaction can be determined by a mode with smaller amplitude. The

formal justification of the multiband GL expansion can be found in.[18]

A. Example: a superconductor with a passive band

To illustrate the analysis of the coherence lengths presented above, we consider the simple case of a two band superconductor where one of the bands is passive, that is, with a potential of the form

$$F_p = -\alpha_1|\psi_1|^2 + \frac{\beta_1}{2}|\psi_1|^2 + \alpha_2|\psi_2|^2 - \gamma(\psi_1\psi_2^* + \psi_1^*\psi_2) \tag{14}$$

where $\alpha_j, \beta_1, \gamma$ are positive constants. Then F_p is minimized when ψ_1 and ψ_2 have equal phase, and have moduli

$$|\psi_1| = u_1 = \sqrt{\frac{\alpha_1}{\beta_1}\left(1 + \frac{\gamma^2}{\alpha_1\alpha_2}\right)}, \qquad |\psi_2| = u_2 = \frac{\gamma}{\alpha_2}u_1. \tag{15}$$

The mass of the vector field A is

$$\mu_A = e\sqrt{u_1^2 + u_2^2} = eu_1\sqrt{1 + \frac{\gamma^2}{\alpha_2^2}}. \tag{16}$$

The Hessian matrix of F_p about (u_1, u_2) is

$$\mathcal{H} = \begin{pmatrix} 4\alpha_1 + \frac{6\gamma^2}{\alpha_2} & -2\gamma \\ -2\gamma & 2\alpha_2 \end{pmatrix}. \tag{17}$$

It is straightforward to compute explicit expressions for the eigenvalues μ_1^2, μ_2^2 of this matrix. The power series expansion in γ reveals that

$$\mu_1 = 2\sqrt{\alpha_1} + O(\gamma^2), \qquad \mu_2 = \sqrt{2\alpha_2} + O(\gamma^2). \tag{18}$$

Similarly, the normalized eigenvector associated with eigenvalue μ_1^2 is

$$v_1 = \begin{pmatrix} 1 \\ -(2\alpha_1 - \alpha_2)^{-1}\gamma \end{pmatrix} + O(\gamma^2) \tag{19}$$

so the normal modes of fluctuation about the ground state are rotated through a mixing angle

$$\Theta = -(2\alpha_1 - \alpha_2)^{-1}\gamma + O(\gamma^2). \tag{20}$$

In comparison with the uncoupled model ($\gamma = 0$) then, we see that, for small coupling γ the length scales $\lambda = 1/\mu_A, \xi_1 = 1/\mu_1, \xi_2 = 1/\mu_2$ are unchanged to leading order, but the normal modes with which $1/\mu_1, 1/\mu_2$ are associated are mixed to leading order. In particular, there are large regions of parameter space where $\mu_2 < \mu_A < \mu_1$, so that vortices attract at long range, even though the active band, ψ_1, is naively "type-2' (that is, $\beta_1 > e^2/4$).

IV. CRITICAL COUPLING (BOGOMOLNYI POINT)

Although it is not related to the topic of this paper, in this section we briefly review Bogomolnyi point physics. In single-component superconductors, the type-1 and type-2 regimes are separated by a Bogomolnyi point $\kappa_c = 1$ (note, again that above we absorbed the factor $1/\sqrt{2}$ into the definition of coherence length, for this reason the critical coupling is different from $1/\sqrt{2}$). At that point vortices do not interact, the free energy of normal-to-superconductor interfaces is zero and we have $H_{c1} = H_{c2} = H_c$.[6,52,54,55] This regime is referred to as the "critical point" because of the saturation of Bogomolnyi inequality.[6,52,54–57] The necessary but not sufficient conditions for a critical point is lack of intervortex forces at long range within the linear approximation. To that end all modes excited in a vortex solution, must have equal masses μ_i. From eq. (12) it is obvious that for a multicomponent superconductor it requires a fine-tuning and in general type-1 and type-2 regimes are not separated by a critical point. Furthermore from the section on microscopic theory below it is clear that in general μ_1 and μ_2 (as functions of system's parameters and temperature) do not cross but form an avoided crossing. Thus in the two-component case the Bogomolnyi critical point is a zero-measure parameter set which requires special symmetry of the model. Such a fine tuning for a composite vortex can be achieved in $U(1) \times U(1)$ system with a potential that is symmetric with respect to both components

$$F_p = -\alpha|\psi_1|^2 + \frac{\beta}{2}|\psi_1|^2 - \alpha|\psi_2|^2 + \frac{\beta}{2}|\psi_2|^2 \tag{21}$$

For a standard form of gradient terms this potential gives equal coherence lengths. The Bogomolnyi point is realised when $\xi_1 = \xi_2 = \lambda$, just like in single-component system vortices do not interact in this regime.

The lack of interaction between vortices at Bogomolnyi point originates in exact cancelation of electromagnetic and core-core interaction. However some weak interaction indeed appear beyond the Ginzburg-Landau theory e.g. by non-locality effects, as was studies in detail single-component models.[58–61] This opens up a narrow window in the parameter space near $\kappa \approx 1$ where the interaction, as was suggested by Eilenberger and studies in detail by Jacobs et al is non-monotonic and in general depends on microscopic detail.[58–60] The simplest approach that was used to investigate the $\kappa \approx 1$ regime was to carry single-component GL expansion to next to leading order in $\tau = 1 - T/T_c$ and gradients.[62,63] However to estimate width of the region, full microscopic theory is need. This was studied in.[58–61]

In two-band superconductors similar "near-Bogomolnyi" regime can be realised in the regimes where there are two-bands but there is no second coherence length and system is characterized by a single parameter $\kappa \approx 1$ [such situations appear e.g. when there is strong interband coupling[18,22]]. Two-band microscopic theory confirmed that the intervortex interaction that play role in "near-Bogomolnyi" regime in single-component model, are important only in the narrow window of $\kappa \approx 1$ in two-band materials well characterized by single κ and is negligible otherwise. The multi-band materials where this physics should be relevant for intervortex interaction should have $\kappa \approx 1$ and $H_{c1} \approx H_{c2}$. These microscopic corrections cannot give observable intervortex attraction of materials like the introduction MgB_2 and Sr_2RuO_4.

In the type-1.5 regime the dominant intervortex forces have different origin and the effects responsible for intervortex forces in the "near-Bogomolnyi" point (non locality etc) are not important. For a comparative study of this physics in multiband materials, full microscopic theory is required that accounts both for multiple coherence lengths and nonlocal effects. It was presented in,[22] certain aspects of it are discussed in the section below.

V. MICROSCOPIC THEORY OF TYPE-1.5 SUPERCONDUCTIVITY IN $U(1)$ MULTIBAND CASE

In this section we briefly outline microscopic theory of type-1.5 superconductivity in the particular case of clean multi-band superconductors that break only $U(1)$ symmetry. In this case existence of multiple coherence lengths does not follow from symmetry and has to be justified. A reader who is interested in more general cases of higher symmetry breaking as well the general properties of the type-1.5 state can skip this discussion and proceed directly to the next section. Existence of multiple superconducting bands is not a necessary condition for appearance of multiple coherence lengths.[22] The appearance of multiple coherence lengths and type-1.5 regime in multiband-band superconductors was described using microscopic theory at all temperatures, without relying on GL expansions in.[22] We refer a reader, interested in a full microscopic theory that does not rely on GL expansion to that work, while here we mainly focus on microscopic justification of GL expansion.

As discussed above, in multi-band systems, in general multi-component GL expansions are not based on symmetry (indeed it is a particular example when a soft explicit breaking of a higher symmetry does not necessarily eliminate classical-field-theoretic description of non-critical modes). Therefore obviously it cannot be obtained as an expansion in a single small parameter $\tau = 1 - T/T_c$.

Instead such expansions are justified when the system has multiple small parameters which are not symmetry-related. In the simplest case these are multiple small gaps in different bands, small gradients, and small interband coupling constants. A single-parameter-τ expansion emerges as a single-component reduction of the model in the $\tau \to 0$ limit for a system that breaks only $U(1)$ symmetry.[18]

In this section we focus on two-band case and consider the microscopic origin of two-component GL model (TCGL) described by the following free energy density:

$$F = \sum_{j=1,2} \left(a_j |\Delta_j|^2 + \frac{b_j}{2} |\Delta_j|^4 + K_j |\boldsymbol{D}\Delta_j|^2 \right) - \gamma \left(\Delta_1 \Delta_2^* + \Delta_2 \Delta_1^* \right) + \frac{B^2}{8\pi} \tag{22}$$

where $\boldsymbol{D} = \boldsymbol{\nabla} + i\boldsymbol{A}$, $\boldsymbol{A}$ and $\boldsymbol{B}$ are the vector potential and magnetic field and $\Delta_{1,2}$ are the gap functions in two different bands.

A. Microscopic model for $U(1)$ two-band system.

To verify applicability of TCGL theory we consider the microscopic model of a clean superconductor with two overlapping bands at the Fermi level.[18,22] Within quasiclassical approximation the band parameters characterizing the two different cylindrical sheets of the Fermi surface are the Fermi velocities V_{Fj} and the partial densities of states (DOS) ν_j, labelled by the band index $j = 1, 2$.

It is convenient to normalize the energies to the critical temperature T_c and length to $r_0 = \hbar V_{F1}/T_c$. The vector potential is normalized by $\phi_0/(2\pi r_0)$, the current density normalized by $c\phi_0/(8\pi^2 r_0^3)$ and therefore the magnetic field is measured in units $\phi_0/(2\pi r_0^2)$ where $\phi_0 = \pi\hbar c/e$ is the magnetic flux quantum. In these units the Eilenberger equations for quasiclassical propagators take the form

$$\begin{aligned} v_{Fj} \boldsymbol{n}_p \boldsymbol{D} f_j + 2\omega_n f_j - 2\Delta_j g_j = 0, \\ v_{Fj} \boldsymbol{n}_p \boldsymbol{D}^* f_j^+ - 2\omega_n f_j^+ + 2\Delta_j^* g_j = 0. \end{aligned} \tag{23}$$

Here $v_{Fj} = V_{Fj}/V_{F1}$, $\omega_n = (2n+1)\pi T$ are Matsubara frequencies, the vector $\boldsymbol{n}_p = (\cos\theta_p, \sin\theta_p)$ parametrizes the position on 2D cylindrical Fermi surfaces. The quasiclassical Green's functions in each band obey normalization condition $g_j^2 + f_j f_j^+ = 1$.

The self-consistency equation for the gaps is

$$\Delta_i = T \sum_{n=0}^{N_d} \int_0^{2\pi} \lambda_{ij} f_j d\theta_p. \tag{24}$$

The coupling matrix λ_{ij} satisfies the symmetry relations $n_1\lambda_{12} = n_2\lambda_{21}$ where n_i are the partial densities of states normalized so that $n_1 + n_2 = 1$. The vector potential satisfies the Maxwell equation $\nabla \times \nabla \times \boldsymbol{A} = \boldsymbol{j}$ where the current is

$$\boldsymbol{j} = -T \sum_{j=1,2} \sigma_j \sum_{n=0}^{N_d} Im \int_0^{2\pi} \boldsymbol{n}_p g_j d\theta_p. \tag{25}$$

The parameters σ_j are given by $\sigma_j = 4\pi\rho n_j v_{Fj}$ and $\rho = (2e/c)^2 (r_0 V_{F1})^2 \nu_0$.

First we can use the microscopic model formulated above to check if it is consistent with the basic feature of the multicomponent GL theory, namely the existence of several distinct coherence lengths. For that purpose we calculate asymptotics of gap functions $|\Delta_{1,2}|(r)$ linearizing the systems of Eilenberger equations (23) together with the self-consistency equation (24). In momentum representation this linear system has a discrete and continuous spectrum of imaginary eigenvalues which determine the inverse decay scales of the gap functions deviations from the ground state.[22] The discrete eigenvalues correspond to the masses of gap functions fields (i.e. the inverse of coherence lengths associated with the linear combinations of the fields as in the previous sections). Besides that there is a continuous spectrum which contains all scales lying on the branch cut going along the imaginary axis starting at $\min_k 2\left(\sqrt{|\Delta_k|^2 + (\pi T)^2}/v_{Fk}\right)$.

The examples from ref.[22] of the temperature dependencies of the masses $\mu_{L,H}(T)$ are shown in the Fig.2. The evolution of the masses $\mu_{L,H}$ is shown in the sequence of plots Fig.2(a)-(d) for λ_J increasing from the small values $\lambda_J \ll \lambda_{11}, \lambda_{22}$ to the values comparable to intraband coupling $\lambda_J \sim \lambda_{11}, \lambda_{22}$. The regime with two massive modes is exactly the same as the given by a two-component GL theory. In this model, at very low temperatures there exists only one massive mode $\mu_L(T)$ lying below the branch cut. As the interband coupling is increased above some critical value the mass $\mu_H(T)$ disappears at all temperatures. In such a regime the asymptotic is determined by a single coherence length and a branch cut with a continuous spectrum of scales. The branch cut contribution is essentially a non-local effect which is not captured by GL theory. Therefore one can expect growing discrepancies between effective GL solution and the result of microscopic theory at low temperatures.

Besides justifying the predictions of phenomenological two-component GL theory[18] the microscopic formalism developed in Ref.([22]) allows to describe type-1.5 superconductivity beyond the validity of GL models. As shown on Fig.3a the function $\mu_L(T)$ is *non-monotonic* at low temperatures. Therefore for a certain range of parameters in contrast with the physics of singe-band superconductors the product of London penetration depth Λ and μ_L has a strong and nonmonotonic temperature dependence making intervortex attraction possible if $\Lambda\mu_L < 1$.

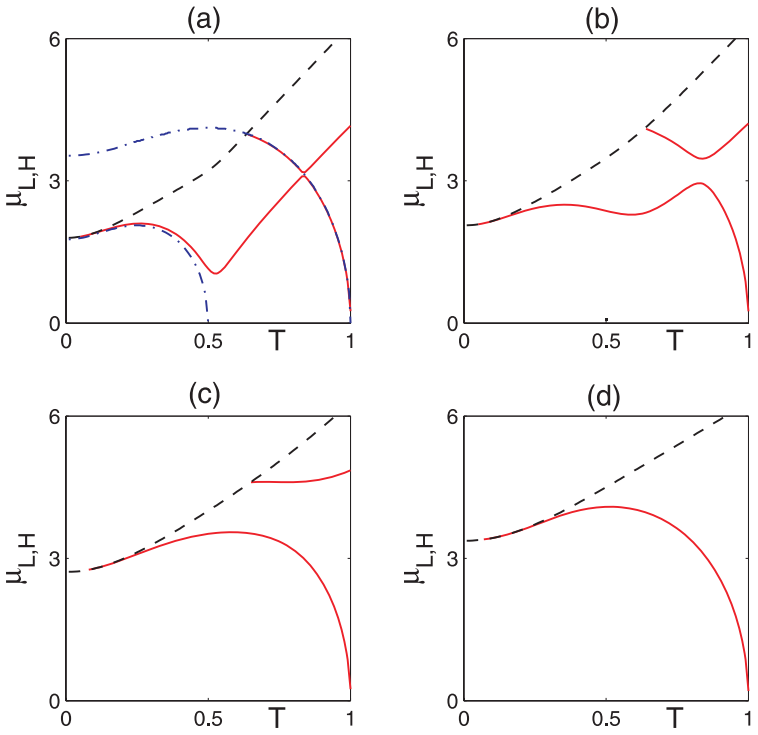

FIG. 2. Calculated in[22] the inverse of coherence lengths (or masses) μ_L and μ_H (red solid lines) of the composite gap function fields for the different values of interband Josephson coupling λ_J and $v_{Fk} = 1$. By black dash-dotted lines the branch cuts are shown. The coupling constants are $\lambda_{11} = 0.25$, $\lambda_{22} = 0.213$ and $\lambda_J = 0.0005;\ 0.0025;\ 0.025;\ 0.213$ for plots (a-d) correspondingly. In (a) the blue dash-dotted lines correspond to $\lambda_J = 0$ showing two masses going to zero at two different temperatures. This corresponds to $U(1) \times U(1)$ theory with two coherence lengths that diverge at different temperatures. For $\lambda_J \neq 0$ only μ_L goes to zero at T_c: this is a consequence of the fact that Josephson coupling breaks the symmetry explicitly down to single $U(1)$ and thus there can be only one diverging coherence length. As one can see from the panels (a)-(c) the $U(1)$ system nonetheless has two well-defined coherence lengths in these regimes, that implies that there are two characteristic length scales in spatial variations of two different linear combinations of fields. When symmetry breaking is weak there is a local maximum of the larger coherence lengths (local minimum of μ_L) at lower temperature (panels (a) and (b)).

To demonstrate the type-1.5 superconductivity i.e. large-scale attraction and small-scale repulsion of vortices which originates from disparity of two coherence lengths, the inter-vortex interaction energy E_{int} was calculated in.[22] In Fig.3(c,d) E_{int} (normalized to the single vortex energy E_v) is shown as a function of the distance between two vortices d. The plots on Fig.3(c) clearly demonstrate the emergence of type-1.5 behavior when the parameter $\gamma_F = v_{F1}/v_{F2}$, which characterizes the disparity in band characteristics is increased.

The type-1.5 regime manifested in the appearance a non-monotonic behavior of $E_{int}(d)$ when

one of the coherence length becomes larger than the magnetic field penetration length. The Fig.3(d) shows E_{int} for a $U(1)$ two band superconductor that is type-2 near T_c and becomes type-1.5 near the temperature where one band crosses over from interband-proximity-effect-induced to intrinsic superconductivity. The long-range attractive forces in type-1.5 regime are similar to the long-range forces in type-1 superconductors, while short-range forces are similar to those in type-2 superconductors. The physical origin and form of these interactions are obviously principally different from the discussed in section IV microscopic-physics and non-locality-dominated intervortex forces in superconductors near Bogomolnyi point.

B. Microscopic Ginzburg-Landau theory for $U(1)$ two-band system.

Here we briefly outline the derivation of TCGL functional (22) from the microscopic equations following.[18] First we find the solutions of Eilenberger Eqs.(23) in the form of the expansion by the amplitudes of gap functions $|\Delta_{1,2}|$ and their gradients $|(\boldsymbol{n}_p\boldsymbol{D})\Delta_{1,2}|$. Then these solutions are substituted to the self-consistency Eq.(24). Using this procedure we find the solutions of Eqs.(23) in the form:

$$f_j = \frac{\Delta_j}{\omega_n} - \frac{|\Delta_j|^2\Delta_j}{2\omega_n^3} - \frac{v_{Fj}}{2\omega_n^2}(\boldsymbol{n}_p\boldsymbol{D})\Delta_j + \frac{v_{Fj}^2}{4\omega_n^3}(\boldsymbol{n}_p\boldsymbol{D})(\boldsymbol{n}_p\boldsymbol{D})\Delta_j. \tag{26}$$

and $f_j^+(\boldsymbol{n}_p) = f_j^*(-\boldsymbol{n}_p)$. Note that this GL expansion is based on neglecting the higher-order terms in powers of $|\Delta|$ and $|(\boldsymbol{n}_p\boldsymbol{D})\Delta|$. Indeed this approximation naturally fails in a number of cases. The regimes when it can be justified were determined in the work[18] by a direct comparison to the full microscopic model. Let us determine microscopic coefficients in the GL expansion. Substituting to the self-consistency Eqs.(24) and integrating by θ_p we obtain

$$\Delta_1 = (\lambda_{11}\Delta_1 + \lambda_{12}\Delta_2)G + (\lambda_{11}GL_1 + \lambda_{12}GL_2) \tag{27}$$

$$\Delta_2 = (\lambda_{21}\Delta_1 + \lambda_{22}\Delta_2)G + (\lambda_{21}GL_1 + \lambda_{22}GL_2) \tag{28}$$

where

$$G = 2\sum_{n=0}^{N_d}\frac{\pi T}{\omega_n}; \quad X = \sum_{n=0}\frac{\pi T}{\omega_n^3} \tag{29}$$

$$GL_j = X\left(\frac{v_{Fj}^2}{4}\boldsymbol{D}^2\Delta_j - |\Delta_j|^2\Delta_j\right) \tag{30}$$

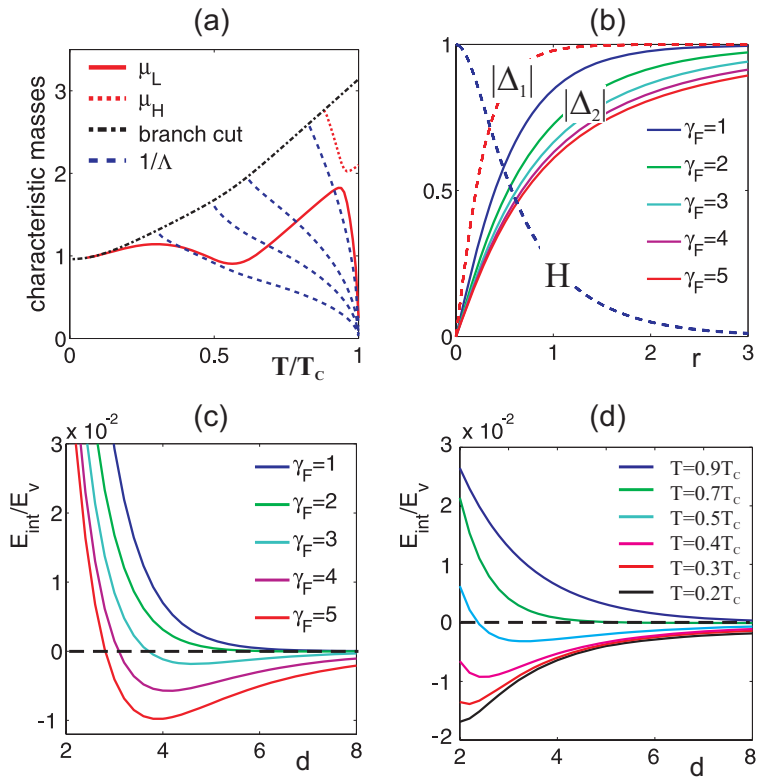

FIG. 3. Calculated in ref.[22] (a) the inverse of coherence lengths (or masses) μ_L and μ_H (red solid and dotted lines) of the composite gap function fields and inverse London penetration (blue dashed lines) for the different values of $\Lambda\mu_L(T_c)/\sqrt{2} = 1; 2; 3; 5$. Scales above the black dash-dotted line are contained in a branch-cut contribution. (b) Distributions of magnetic field $H(r)/H(r=0)$, gap functions $|\Delta_1|(r)/\Delta_{10}$ (dashed lines) and $|\Delta_2|(r)/\Delta_{20}$ (solid lines) for the coupling parameters $\lambda_{11} = 0.25$, $\lambda_{22} = 0.213$ and $\lambda_{21} = 0.0025$ and different values of the band parameter $\gamma_F = 1; 2; 3; 4; 5$. (c,d) The interaction energy E_{int} between two vortices normalized to the single vortex energy E_v as function of the intervortex distance d. In panel (c) the pairing constants are the same as in (d) and $T = 0.6T_c$. In panel (d) λ_{ii} are the same as in (c) but $\lambda_{21} = 0.00125$, and $\gamma_F = 1$. The panel (d) shows that when, at lower temperature, one of the coherence lengths becomes larger than the magnetic field penetration length, the system falls into type-1.5 regime. The strength on the attraction grows as temperature becomes lower. The inter vortex distance corresponding to minimum of interaction potential is strongly temperature dependent even below $0.5T_c$. It diminishes when temperature is decreased which should result in vortex cluster shrinkage with decreasing temperature.

Expressing GL_i from the equations above we obtain

$$n_1 GL_1 = n_1 \left(\frac{\lambda_{22}}{\mathrm{Det}\hat{\Lambda}} - G \right) \Delta_1 - \frac{\lambda_J n_1 n_2}{\mathrm{Det}\hat{\Lambda}} \Delta_2 \tag{31}$$

$$n_2 GL_2 = n_2 \left(\frac{\lambda_{11}}{\mathrm{Det}\hat{\Lambda}} - G \right) \Delta_2 - \frac{\lambda_J n_1 n_2}{\mathrm{Det}\hat{\Lambda}} \Delta_1 \tag{32}$$

The system of two coupled GL Eqs.(31) can be obtained minimizing the free energy provided the coefficients in Eq.(22) are given by

$$a_i = \rho n_i(\tilde{\lambda}_{ii} + \ln T - G_c) \tag{33}$$
$$\gamma = \rho n_1 n_2 \lambda_J / \mathrm{Det}\hat{\Lambda}$$
$$b_i = \rho n_i X/T^2$$
$$K_i = v_{Fi}^2 b_i/4$$

where $\lambda_J = \lambda_{21}/n_1 = \lambda_{12}/n_2$. Note that the expression for K_i in Ref.[18] an extra coefficient ρ. The temperature is normalized to the T_c. Here $X = 7\zeta(3)/(8\pi^2) \approx 0.11$, $\bar{\lambda}_{ij} = \lambda_{ij}^{-1}$ and $G_c = G(T_c)$ is determined by the minimal positive eigenvalue of the inverse coupling matrix $\hat{\lambda}^{-1}$:

$$G_c = \frac{\mathrm{Tr}\lambda - \sqrt{\mathrm{Tr}\lambda^2 - 4\mathrm{Det}\lambda}}{2\mathrm{Det}\lambda}.$$

We have used the expression $G(T) = G(T_c) - \ln T$. Near the critical temperature $\ln T \approx -\tau$ and we obtain

$$a_i = \alpha_i(T - T_i) \tag{34}$$
$$\alpha_i = n_i \lambda_J \tag{35}$$
$$T_i = (1 + G_c - \tilde{\lambda}_{ii}). \tag{36}$$

In the above procedure of GL expansion leading to the system (31) we assumed both the eigenvalues of the coupling matrix $\hat{\lambda}$ are positive.

C. Temperature dependence of coherence lengths.

Coherence lengths are given by the inverse masses of linear modes. First we investigate the asymptotic behaviour of the superconducting gaps formulated in terms of the linear modes of the density fields both in TCGL and microscopic theories described in the previous section. To find the linear modes we follow the procedure described in the section (III) using the GL model with expansion coefficients (33). Let us set $K_1 = K_2$ which can be accomplished by rescaling the fields $\Delta_{1,2}$. Then the corresponding Hessian matrix (5) can be diagonalized with the k-independent rotation introducing the normal modes $\chi_\beta = U_{\beta i}(\Delta_i - \Delta_{i0})$ where $\beta = L, H$ and $i = 1, 2$. The rotation matrix $\hat{U}$ is characterized by the mixing angle[7,22] as follows:

$$\hat{U} = \begin{pmatrix} \cos\theta_L & \sin\theta_L \\ -\sin\theta_H & \cos\theta_H \end{pmatrix} \tag{37}$$

Note that in accordance with the results of section (III) the TCGL theory yields identical values of two mixing angles $\theta_L = \theta_H = \Theta$ where Θ is given by the Eq.(20). However, in general, outside the region where GL expansion is accurate, the exact microscopic calculation of asymptotic yields deviations $\theta_H \neq \theta_L$. This is discussed in Ref.[18]

The fields $\chi_{L,H}$ corresponding to the linear combinations of $\Delta_{1,2}$ vary at distinct lengths: $\xi_H = 1/\mu_H$ and $\xi_L = 1/\mu_L$. They constitute coherence lengths of the TCGL theory (22) and characterize the asymptotic relaxation of the linear combinations of the fields $\Delta_{1,2}$, the linear combinations are represented by the composite fields $\chi_{L,H}$.

With the help of Eqs.(33) for GL coefficients obtained from microscopic theory we can study the temperature dependencies of the coherence lengths characterizing the asymptotic relaxation of the gap fields and compare them to the temperature dependence of coherence lengths in full microscopic theory. Since the system in question breaks only one symmetry, then at critical temperature only one coherence length can diverge while the second coherence should stay finite. Infinitesimally close to critical temperature $T = T_c - 0$ the divergent coherence length has the following standard mean-field behavior $\xi_L = 1/\mu_L \sim 1/\tau^{1/2}$, where $\tau = 1 - T/T_c$. The contribution of another linear mode in the theory sets the scale which is proportional to $\xi_H = 1/\mu_H$. It remains finite at $T = T_c$. But the amplitude of this mode rapidly vanishes in that region $T = T_c - 0$. In Fig.(4)a,b the temperature dependence of masses $\mu_{L,H}$ is plotted comparing the results of the full microscopic[22] and microscopically derived TCGL theories.[18] It is shown for the cases of weak and strong interband coupling in Fig.(4)c,d. We have found that TCGL theory describes the lowest characteristic mass $\mu_L(T)$ (i.e. the longer coherence length) with a very good accuracy near T_c [compare the blue and red curves in Fig. (4)a,b]. Remarkably, when interband coupling is relatively weak [Fig.(4)c] the "light" mode is quite well described by TCGL also at low temperatures down to $T = 0.5T_c$ around which the weak band crosses over from active to passive (proximity-induced) superconductivity. Indeed the τ parameter is large in that case. Nonetheless if the interband coupling is small one does have a small parameter to implement a GL expansion for one of the components. Namely one can still expand, e.g. in the powers of the weak gap $|\Delta_2|/\pi T \ll 1$. On the other hand for the "heavy" mode we naturally obtain some discrepancies even relatively close to T_c, although TCGL theory gives qualitatively correct picture for this mode when the interband coupling is not too strong. More substantial discrepancies between TCGL and microscopic theories appear only at lower temperatures or at stronger interband coupling [Fig.(4)d] where the microscopic response function has only one pole, while TCGL theory generically has two poles. Note that these expected deviations concern shorter-range physics and do not directly affect long-range intervortex forces. In

the type-1.5 regime long-range attractive forces are governed by core-core interaction which range is set by the larger coherence length (lighter mode).

The microscopic two-band GL expansion discussed in this section has straightforward generalization to N-component expansions in N-band $U(1)$ models.[49] For a discussion of microscopic GL expansion in more complicated states such as $s + is$ that break multiple symmetries see.[9,49]

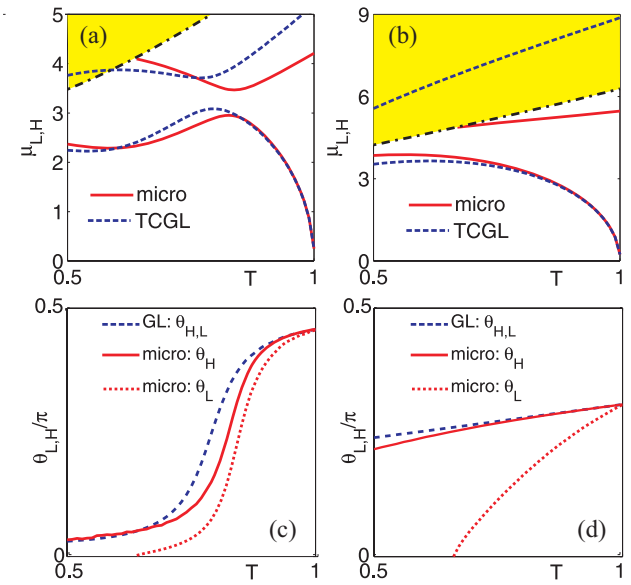

FIG. 4. (a) and (b) Comparison of field masses (inverse coherence lengths) given by full microscopic (solid lines), and microscopically-derived TCGL (dotted) theories. The microscopic parameters are $\lambda_{11} = 0.5$, $\lambda_{22} = 0.426$ and $\lambda_{12} = \lambda_{21} = 0.01$; 0.1 for (a,b) correspondingly. The yellow shaded region above the dashed-dotted line shows the continuum of length scales determined by a branch-cut contributions which are specific to the microscopic theory and are not captured by the TCGL description. (c,d) Comparison of the mixing angle behaviour given by the exact microscopic (red lines) and microscopically derived TCGL theories (blue line). Note that the larger coherence length has a maximum as a function of temperature deep below T_c near the crossover to the regime when the weak band superconductivity is induced by an interband proximity effect (the corresponding inverse quantity μ_L has a minimum). This non-monotonic coherence length behavior is more pronounced at weak interband coupling and disappears at strong interband coupling.[22] A multiband system with weak interband interaction can easily fall into type-1.5 regime near that crossover temperature. Panels (b) and (d) show a pattern how the TCGL theory starts to deviate from the microscopic theory at lower temperature when interband coupling is increased. Parameters are the same as on the panels (a,b) correspondingly.

VI. SYSTEMS WITH GENERIC BREAKDOWN OF TYPE-1/TYPE-2 DICHOTOMY

In this section we discuss the simplest situations of generic type-1/type-2 dichotomy breakdown. One example is superconducting systems that exhibit a phase transition from $U(1)$ to $U(1) \times U(1)$ state (or similar transitions between the states with broken higher symmetries), such as the theoretically discussed superconducting states of liquid metallic hydrogen or deuterium,[11] or models involving mixture of protonic and Σ^- hyperonic condensates in neutron stars,[13] as well as microscopic certain interface superconductors.[33] Indeed at such a transition the magnetic field penetration length remains finite but there is a divergent coherence length due to the breakdown of additional symmetry (if the phase transition is continuous). Also the mode associated with the divergent coherence length looses its amplitude at the phase transition. Therefore near this transition one of the coherence lengths is the largest length scale of the problem and the system can only be either a type-1 or type-1.5 superconductor.

Similar but more subtle situation takes place at the transition from s to $s+is$ state.[10] The $s+is$ superconductor breaks additional Z_2 symmetry and there is a corresponding diverging coherence length in the problem. An important generic aspect of the $s+is$ superconducting states is that the density excitations are coupled with the phase difference excitations in the linear theory.[10] One of the mixed phase-difference–density mode gives raise to a divergent coherence length at that phase transition. Thus such a system can be either type-1 or type-1.5 near the transition from s to $s+is$ state. We discuss this example in more detail in Section VIII.

VII. STRUCTURE OF THE VORTEX CLUSTERS IN TYPE-1.5 TWO-COMPONENT SUPERCONDUCTOR.

In this section, following Ref.[23] we consider in more detail the full non-linear problem in two-component Ginzburg-Landau models, with and without Josephson coupling η which directly couples the two condensates (for treatment of other kinds of interband couplings see,[7] for microscopic derivation of the coefficients see Sec.IV). When $\eta = 0$ the condensates are coupled electromagnetically. When there is non-zero interband Josephson coupling, the phase difference is associated with a massive mode with mass $\sqrt{\eta(u_1^2+u_2^2)/u_1u_2}$.

$$\mathcal{F} = \frac{1}{2}\sum_{i=1,2}\left[|(\nabla + ie\mathbf{A})\psi_i|^2 + (2\alpha_i + \beta_i|\psi_i|^2)|\psi_i|^2\right] + \frac{1}{2}(\nabla\times\mathbf{A})^2 - \eta|\psi_1||\psi_2|\cos(\theta_2-\theta_1) \quad (38)$$

Since the Ginzburg-Landau model is non-linear, in general intervortex interaction is non-pairwise. Non-pairwise interaction are important at shorter ranges where linearised theory, consid-

ered above, does not in general apply. Below we discuss the importance of complicated non-pairwise forces between superconducting vortices arising in certain cases in multicomponent systems.[23,43,44] These non-pairwise forces in certain cases have important consequences for vortex clusters formation in the type-1.5 regime.

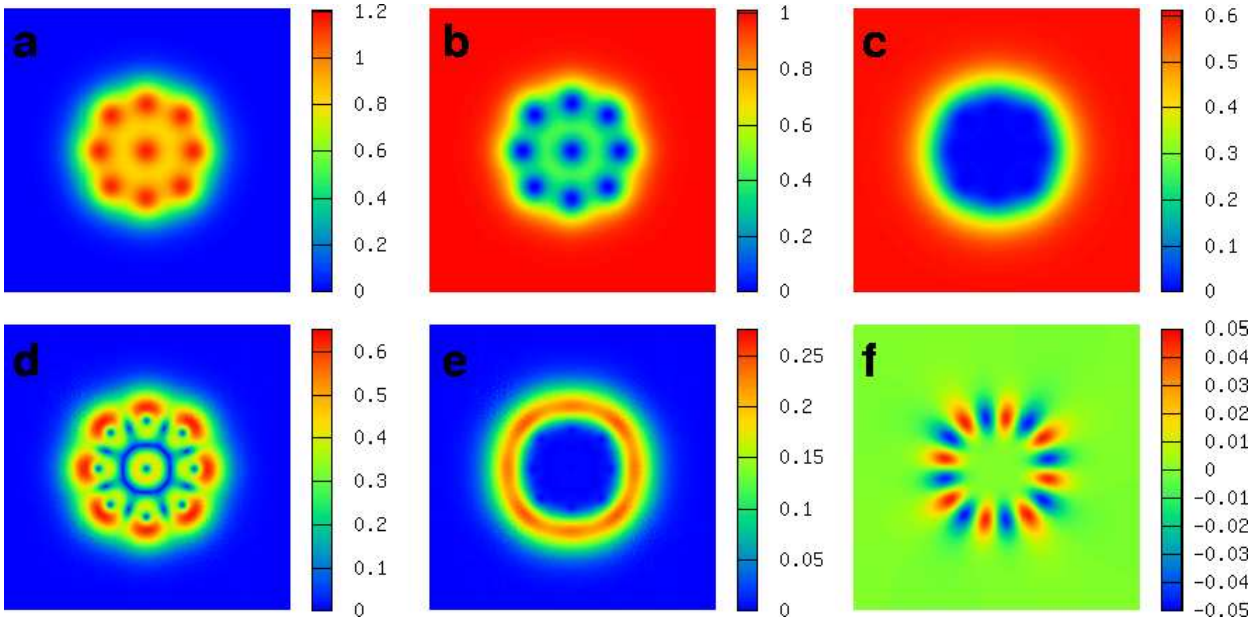

FIG. 5. Ground state of $N_v = 9$ flux quanta in a $U(1) \times U(1)$ type-1.5 superconductor (*i.e.* $\eta = 0$). The parameters of the potential being here $(\alpha_1, \beta_1) = (-1.00, 1.00)$ and $(\alpha_2, \beta_2) = (-0.60, 1.00)$, while the electric charge is $e = 1.48$ (in these units the electric charge value parameterises London penetration length). The displayed physical quantities are **a** the magnetic flux density, **b** (*resp.* **c**) is the density of the first (*resp.* second) condensate $|\psi_{1,2}|^2$. **d** (*resp.* **e**) shows the norm of the supercurrent in the first (*resp.* second) component. Panel **f** is $\mathrm{Im}(\psi_1^* \psi_2) \equiv |\psi_1||\psi_2| \sin(\theta_2 - \theta_1)$ being nonzero when there appears a difference between the phase of two condensates. The solution shows that clearly there is vortex interaction-induced phase-difference gradient which contributes to non-pairwise intervortex forces. Parameters are chosen so that the second component has a type-1 like behavior while the first one tends to from well separated vortices. The density of the second band is depleted in the vortex cluster and its current is mostly concentrated on the boundary of the cluster (see Ref.[23]).

Fig. 5 and Fig. 6 show numerical solutions for N-vortex bound states in several regimes (for technical details see Appendix of[23]). The common aspect of the regimes shown on these figures is that the density of one of the components is depleted in the vortex cluster and has its current mostly concentrated on the boundary of the vortex cluster (i.e. has a "type-1"-like behavior). At the same time the second component forms a distinct vortex lattice inside the vortex cluster (i.e. has a "type-2"-like behavior).

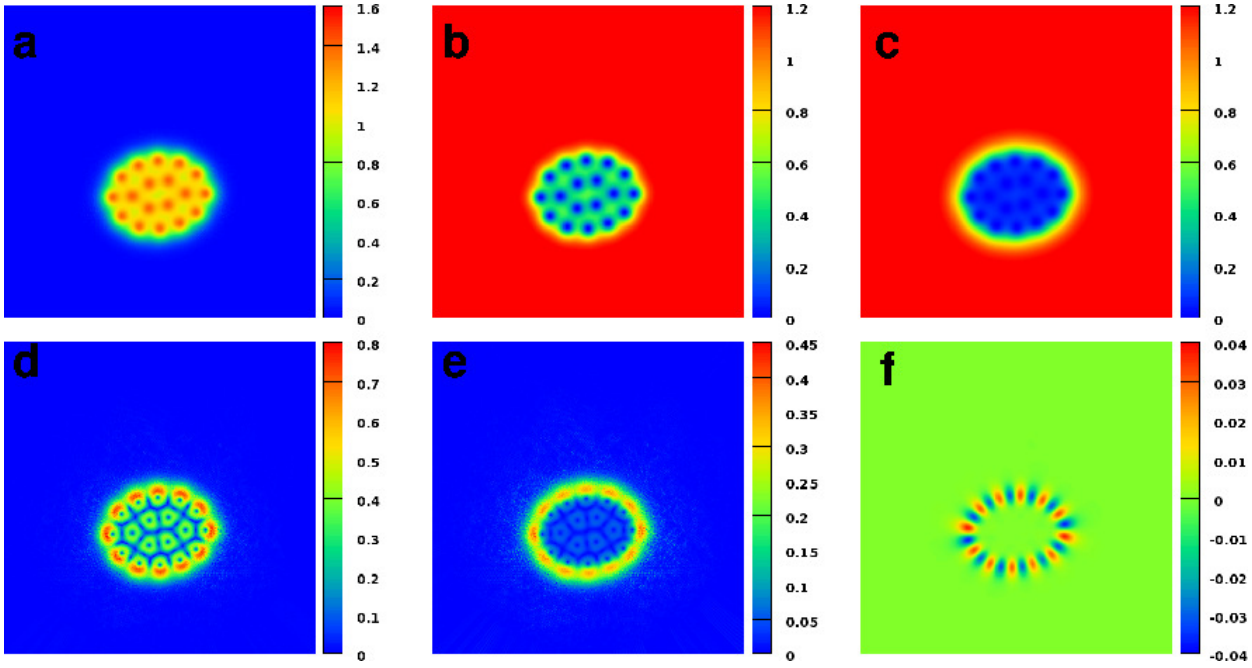

FIG. 6. Elongated ground state cluster of 18 vortices in a superconductor with two active bands. Parameters of the interacting potential are $(\alpha_1, \beta_1) = (-1.00, 1.00)$, $(\alpha_2, \beta_2) = (-0.0625, 0.25)$ while the interband coupling is $\eta = 0.5$. The electric charge, parameterizing the penetration depth of the magnetic field, is $e = 1.30$ so that the well in the nonmonotonic interacting potential is very small. In this case there is visible admixture of the current of second component in vortices inside the cluster, though its current is predominantly concentrated on the boundary of the cluster.

Next we report the regime where the passive second band (i.e. with positive α_2) is coupled to the first band by strong Josephson coupling $\eta = 7.0$ (shown on Fig. 7). This coupling imposes a strong energy penalty both for disparities of the condensates variations and for the difference between phases of the condensates. In this regime there are also relatively strong non-pairwise intervortex forces favouring chain-like vortex arrangements compared to compact clusters.[23] We get a relatively flat and complicated energy landscape for multi-vortex configurations and the outcome of the energy minimization strongly depends on initial configuration. Simulations whose outcome is compact clusters like Fig. 5 and Fig. 6 are clearly ground states, since various initial guesses lead to similar final configurations. Simulating systems like in Fig. 7 is less straightforward. Numerical evolution in these systems is extremely slow because of the complicated energy landscape. The final state strongly depends on the initial field configuration, indicating the configuration is not the ground state, but a "quasi-stationary" bound state with a very slow evolution. Formation of highly disordered states and vortex chains due to the short-range nature of the attractive potentials and many-body forces was a common outcome of the simulation in similar type-1.5 regimes,[23] in

spite of the use of a fine numerical grid. Another example of systems that are generally more inclined to posses non-pairwise intervortex forces that promote vortex-stripes are superconducting condensates with phase separation.[43]

The Fig. 7 shows the typical non-universal outcome of the energy minimization in this case. A striking feature here is formation of vortex stripe-like configuration, in contrast with the ground state expected from the two-body forces in this system. Namely the axially symmetric two-body potentials with long range attraction and short-range repulsion (which we have in this case) do not allow ground states with stripe formation. In that regime the formation of vortex stripes and small lines is aided by the repulsive non-pairwise intervortex interactions.[23]

Note that even in this regime, the non-linear effects in caused by intervortex interaction result in self-induced gradients of the phase difference, in spite of the strong Josephson coupling.

When stray fields are taken into account in thin films, they give repulsive inter vortex interaction at very long distances, while vortices can retain attractive interaction at intermediated length scales. That gives raise to various hierarchical structures such as lattices of vortex clusters or vortex stripes.[39,64] The study of dynamics demonstrated that such vortex systems can form vortex glass phase.[65] This is in contrast to type-2 superconductors where vortex glass can appear only in the presence of vortex pinning and not in clean samples.

VIII. MACROSCOPIC SEPARATION IN DOMAINS OF DIFFERENT BROKEN SYMMETRIES IN TYPE-1.5 SUPERCONDUCTING STATE.

As discussed above a system with non-monotonic intervortex interaction potentials allow a state with macroscopic phase separation in vortex droplets and Meissner domains. In type-1.5 superconductors this state can also represent a phase separation into domains of states with different broken symmetries. In this section we will give two different examples of how such behavior arises.

Note that in multicomponent superconductors some symmetries are global (i.e. associated with the degrees of freedom decoupled from vector potential) and some are local i.e. associated with the degrees of freedom coupled to vector potential. As is well known, in the later case the concept of spontaneous symmetry breakdown is not defined the same way as in a system with global symmetry. However below, for brevity we will not be making terminological distinctions between local and global symmetries (detailed discussion of these aspects can be found in e.g.[50]).

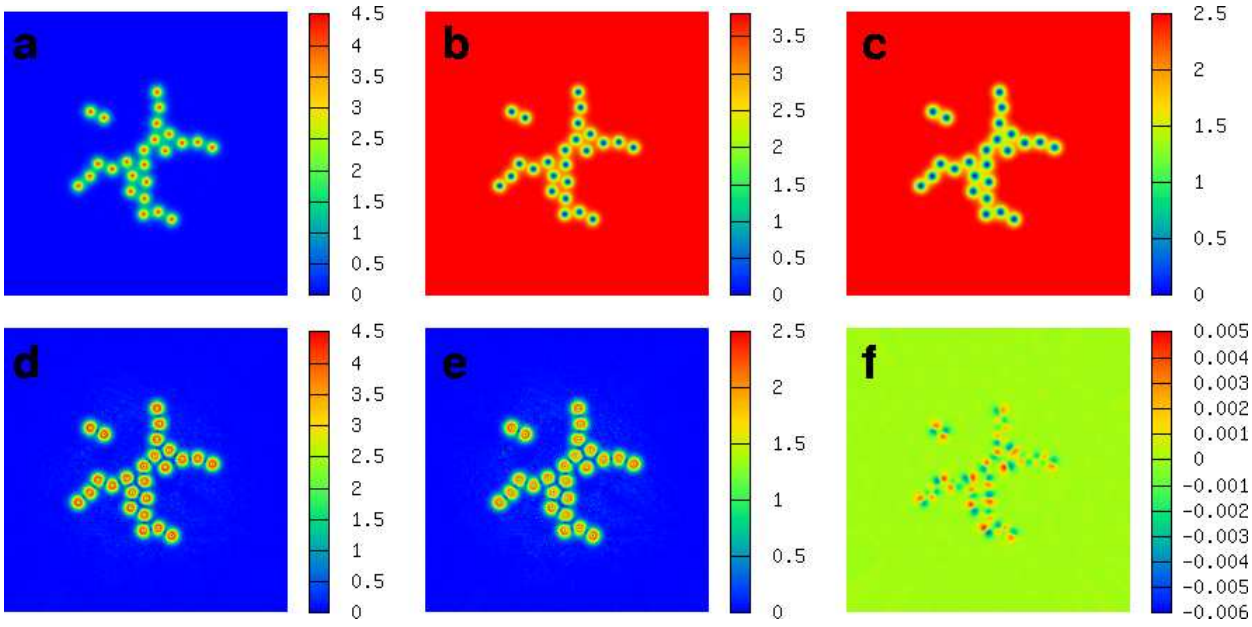

FIG. 7. A bound state of an $N_v = 25$ vortex configuration in case when superconductivity in the second band is due to interband proximity effect and the Josephson coupling is relatively strong $\eta = 7.0$. The initial configuration in this simulation was a giant vortex. Other parameters are $(\alpha_1, \beta_1) = (-1.00, 1.00)$, $(\alpha_2, \beta_2) = (3.00, 0.50)$, $e = 1.30$. For the simulations, like the one shown on Fig. 6 the stopping criterion of energy minimization was when relative variation of the norm of the gradient of the GL functional with respect to all degrees of freedom to be less than 10^{-6}. Here the situation is slightly different from that shown on two previous figures. Clearly in the shown above configuration the ground state was not reached. However the interaction potentials a such that the evolution at the later stages becomes extremely slow. The number of energy minimization steps in this case was order of magnitude larger than what was required for convergence in the previous regimes. This signals that in similar systems vortex stripes will be likely to form (relative to more compact vortex clusters) for kinetic reasons as well as due to thermal fluctuations

A. Macroscopic phase separation into $U(1) \times U(1)$ and $U(1)$ domains in type-1.5 regime.

Consider a superconductor with broken $U(1) \times U(1)$ symmetry, i.e. a collection of independently conserved condensates with no intercomponent Josephson coupling. As discussed above, in the vortex cluster state, in the interior of a vortex droplet, the superconducting component which has vortices with larger cores is more depleted. In $U(1) \times U(1)$ system the vortices with phase windings in different condensates are bound electromagnetically, resulting in an asymptotically logarithmic interaction potential with a prefactor proportional to $|\psi_1|^2|\psi_2|^2/(|\psi_1|^2 + |\psi_2|^2)$,[50] and even weaker interaction strength at shorter separations.

Consider now a macroscopically large vortex domain. Even if the second component there

is not completely depleted, its density is suppressed and as a consequence the binding energy between vortices with different phase windings ($\Delta\theta_1 = 2\pi, \Delta\theta_2 = 0$) and ($\Delta\theta_1 = 0, \Delta\theta_2 = 2\pi$) can be arbitrarily small. Moreover the vortex ordering energy in the component with more depleted density is small as well. As a result, even tiny thermal fluctuation can drive vortex sublattice melting transition[11,66] in a large vortex cluster. In that case the fractional vortices in weaker the component tear themselves off the fractional vortices in strong the component and form a disordered state. Note that the vortex sublattice melting is associated with the phase transition from $U(1)\times U(1)$ to $U(1)$ broken symmetries.[11,66] Thus, a macroscopically large vortex cluster can realise a domain of $U(1)$ phase (associated with the superconducting state of strong component) immersed in domain of vortexless $U(1) \times U(1)$ Meissner state. If the magnetic field is increased, the system will go from the vortex clusters state (with coexisting $U(1) \times U(1)$ and $U(1)$ domains) to a $U(1)$ vortex state.

B. Macroscopic phase separation in $U(1)$ and $U(1) \times Z_2$ domains in three band type-1.5 superconductors.

In this subsection we discuss an example of vortex clusters in three-band superconductors that locally break additional Z_2 symmetry forming "phase-frustrated" states. Such superconductors also allow the coexistence of domains with different broken symmetries in the ground state. The minimal GL free energy functional to model a three-band superconductor is

$$F = \frac{1}{2}(\nabla \times \mathbf{A})^2 + \sum_{i=1,2,3} \frac{1}{2}|\mathbf{D}\psi_i|^2 + \alpha_i|\psi_i|^2 + \frac{1}{2}\beta_i|\psi_i|^4 + \sum_{i=1,2,3}\sum_{j>i} \eta_{ij}|\psi_i||\psi_j|\cos(\varphi_{ij})\,. \qquad (39)$$

Here the phase difference between two components are denoted $\varphi_{ij} = \theta_j - \theta_i$. Microscopic derivations of such models describing $s + is$ superconducting states can be found in.[9,49]

Systems with more than two Josephson-coupled bands can exhibit phase frustration.[8–10,67,68] For $\eta_{ij} < 0$, a given Josephson interaction energy term is minimal for zero phase difference (we then refer to the coupling as "phase-locking"), while when $\eta_{ij} > 0$ it is minimal for a phase difference equal to π (we then refer to the coupling as "phase-antilocking"). Two-component systems with bilinear Josephson coupling are symmetric with respect to the sign change $\eta_{ij} \to -\eta_{ij}$ as the phase difference changes by a factor π, for the system to recover the same interaction. However, in systems with more than two bands there is generally no such symmetry. For example if a three-band system has $\eta > 0$ for all Josephson interactions, then these terms can not be simultaneously minimized, as this would correspond to all possible phase differences being equal to π.

The ground state values of the fields $|\psi_i|$ and φ_{ij} of system (39) are found by minimizing the potential energy

$$\sum_i \left\{\alpha_i|\psi_i|^2 + \frac{1}{2}\beta_i|\psi_i|^4\right\} + \sum_{j>i}\eta_{ij}|\psi_i||\psi_j|\cos(\varphi_{ij}). \tag{40}$$

This can however not be done analytically in general, though certain properties can be derived from qualitative arguments. In terms of the sign of the η's, there are four principal situations:

Case	Sign of $\eta_{12}, \eta_{13}, \eta_{23}$	Ground State Phases
1	$---$	$\varphi_1 = \varphi_2 = \varphi_3$
2	$--+$	Frustrated
3	$-++$	$\varphi_1 = \varphi_2 = \varphi_3 + \pi$
4	$+++$	Frustrated

The case 2) can result in several ground states. If $|\eta_{23}| \ll |\eta_{12}|,\ |\eta_{13}|$, then the phase differences are generally $\varphi_{ij} = 0$. If on the other hand $|\eta_{12}|,\ |\eta_{13}| \ll |\eta_{23}|$ then $\varphi_{23} = \pi$ and φ_{12} is either 0 or π. However in certain parameter ranges the resulting state is in fact a "compromise" where φ_{ij} is not an integer multiples of π.

The case 4) is in fact equivalent to 2) (mapping between these scenarios is trivial). The wide range of resulting groundstates can be seen in Fig. 8. As η_{12} is scaled, ground state phases change from $(-\pi,\ \pi,\ 0)$ to the limit where one band is depleted and the remaining phases are $(-\pi/2,\ \pi/2)$.

An important property of the potential energy (40) is that if any of the phase differences φ_{ij} is not an integer multiple of π, then the ground state posses an additional discrete Z_2 degeneracy. For example for a system with $\alpha_i = -1,\ \beta_i = 1$ and $\eta_{ij} = 1$, two possible ground states exist and are given by $\varphi_{12} = 2\pi/3,\ \varphi_{13} = -2\pi/3$ or $\varphi_{12} = -2\pi/3,\ \varphi_{13} = 2\pi/3$. Thus in this case, the broken symmetry is $U(1) \times Z_2$, as opposed to $U(1)$. As a result, like any other system with Z_2 degeneracy, the theory allows an additional set of topological excitations: domain walls interpolating between the two inequivalent ground states as well as more complicated topological excitations.[69–71] Generalisations to frustrated systems with larger number of components was discussed in.[72]

There is a divergent coherence length at the critical point where the system undergoes the $U(1) \times Z_2 \to U(1)$ phase transition (when there is a second order phase transition from an $s + is$ to an s state). The nature of this divergent length-scale is revealed by calculation of the normal modes. Specifically, generating a set of differential equations from the eq.(39) and linearising these

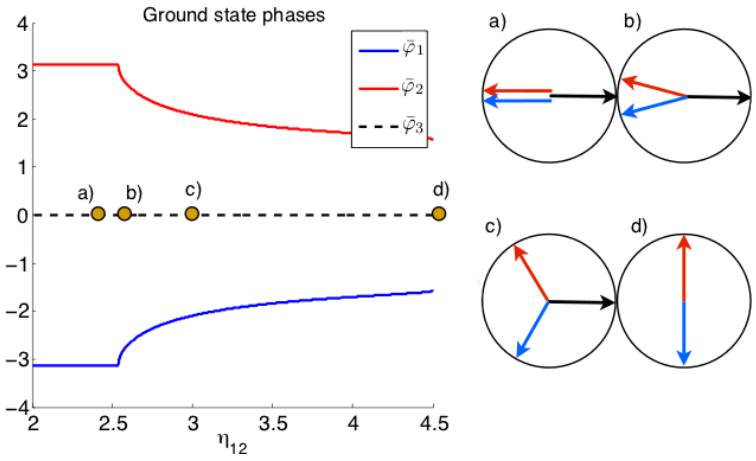

FIG. 8. Ground state phases of the three components as function of η_{12} (here $\theta_3 = 0$ fixes the gauge). The GL parameters are $\alpha_i = 1$, $\beta_i = 1$, $\eta_{13} = \eta_{23} = 3$. For intermediate values of η_{12} the ground state exhibits discrete degeneracy (symmetry is $U(1) \times Z_2$ rather than $U(1)$) since the energy is invariant under the sign change $\theta_2 \to -\theta_2$, $\theta_3 \to -\theta_3$. For large η_{12} we get $\theta_2 - \theta_3 = \pi$ implying that $|\psi_3| = 0$ and so there is a second transition from $U(1) \times Z_2$ to $U(1)$ and only two bands at the point d). Here, the phases were computed in a system with only passive bands, though systems with active bands exhibit the same qualitative properties except for the transition to $U(1)$ and two bands only (*i.e.* active bands have non-zero density in the ground state).

close to the groundstate, gives a mass-matrix whose eigenbasis is also an orthonormal basis of small perturbations to the ground state.[10] In systems that break only $U(1)$ symmetry, these modes are segregated with respect to phase and amplitude so that small perturbations to the phase and amplitude sectors decay independently of each other. Small perturbations to the amplitude thus has no implications for the phase difference sector, and vice versa. In contrast, in the region where Z_2 symmetry is broken the modes are generally mixed in this kind of models. In this case a perturbation to the amplitude sector necessarily implies a perturbation to the phase sector and vice versa.

The immediate implication of this is that in the region with broken Z_2-symmetry, there are five rather than three coherence lengths that describe amplitude perturbations. If the phase transition is second order one of these coherence lengths diverges as we approach the transition point where Z_2-symmetry is restored. Thus, vortices in this region produce a perturbation to the amplitude that recovers with a coherence length that is divergent. Since the magnetic field penetration depth is finite at that transition the system can be either type-1 or type-1.5 with attractive inter-vortex interaction.[10]

In the iron-based superconductors a phase transition from s-wave to $s + is$ state is expected to

take place as a function of doping.[9] Thus, if there is an $s+is$ region at the phase diagram, there should be a range of doping and temperatures in the proximity of the critical point where the type-1.5 superconductivity is generic. The general case of N-component frustrated superconductors is less studied, however certainly in case of larger number of components there are more possibilities for the appearance of normal modes with low or zero masses leading to type-1.5 regimes.[72]

C. Non-linear effects and long-range intervortex interaction in $s+is$ superconductors.

The ground state of a phase frustrated superconductor is in many cases non-trivial, with phase differences being compromises between the various interaction terms. Inserting vortices in such a system can shift the balance between different competing couplings, since vortices can in general have different effects on the different bands. In particular, since the core sizes of vortices are not generally the same in all bands, vortex matter typically depletes some components more than others and thus can alter the preferred values of the phase difference. So the minimal potential energy inside a vortex lattice or cluster may correspond to a different set of phase differences than in the vortex-free ground state. In particular even in s-wave systems vortices can create "bubbles" of Z_2 order parameter around themselves. To see this, consider the following argument: The phase-dependent potential terms in the free energy (39) are of the form

$$\eta_{ij} u_i u_j f_i(\mathbf{r}) f_j(\mathbf{r}) \cos(\varphi_{ij}(\mathbf{r}))\,, \tag{41}$$

where u_i are ground state densities and each $f_i(\mathbf{r})$ represent an Ansatz which models how superfluid densities are modulated due to vortices. Consider now a system where N vortices are uniformly distributed in a domain Ω. The phase dependent part of the free energy is

$$U_\varphi = \left[\sum_{i>j} \eta_{ij} u_i u_j\right] \int_\Omega d\mathbf{r} f_i(\mathbf{r}) f_j(\mathbf{r}) \cos(\varphi_{ij}(\mathbf{r})). \tag{42}$$

If φ_{ij} is varying slowly in comparison with the inter vortex distance, then it can be considered constant in a uniform distribution of vortices (as a first approximation). In that case (42) can be approximated by

$$U_\varphi \simeq \sum_{ij} \tilde{\eta}_{ij} u_i u_j \cos(\varphi_{ij}) \text{ where } \tilde{\eta}_{ij} = \eta_{ij} \int_\Omega d\mathbf{r} f_i(\mathbf{r}) f_j(\mathbf{r}) \tag{43}$$

If on the other hand φ_{ij} varies rapidly, then it is not possible to define $\tilde{\eta}_{ij}$ without a spatial dependence. Then φ_{ij} will depend on $\tilde{\eta}_{ij}(\mathbf{r})$ which is related to the local modulation functions $f_i f_j$ and vary with a characteristic length scale.

Thus, $\tilde{\eta}$ is the effective inter-band interaction coupling resulting from density modulation. Since in general, $f_i \neq f_j$ (unless the two bands i, j are identical), one must take into account the modulation functions f_i when calculating the phase differences. In particular, if the core size in component i is larger than in component j, then $\int d\mathbf{r} f_i f_k < \int d\mathbf{r} f_j f_k$ and therefore the phase differences φ_{ij} minimizing (43) depend on f_i, and consequently on the density of vortices. Thus introducing vortices in the system is, in a way, equivalent to a relative effective decrease of some of the Josephson coupling constants.

This can alter the state of the system, as the symmetry of the problem depends on the Josephson interaction terms. In Figs. 9 , 10 we see a type-1.5 system in which the symmetry of the ground state is $U(1)$. As vortices are inserted into the system, they form clusters and the effective inter band interactions $\tilde{\eta}_{ij}$ are renormalized to a degree that the symmetry of the domain near vortex clusters changes to $U(1) \times Z_2$. Thus the vortex cluster state in such a system represents macroscopic phase separation in domains of broken $U(1)$ and $U(1) \times Z_2$ symmetries.

The vortex structure near the Z_2 phase transition which we discussed in this section has important consequences for the phase diagram of the system beyond mean-field approximation, leading to reentrant phase transitions.[73]

In the vicinity of Z_2 phase transition, besides the appearance of type-1.5 regime, the system has a number of other unusual properties such as anomalous vortex viscosity[74] and distinct anomalous thermoelectric effects.[75,76]

IX. FLUCTUATION EFFECTS IN TYPE-1.5 SYSTEMS

In single-component Ginzburg-Landau models, the order of superconducting transition in zero applied magnetic field in three dimensions depends on the ratio of magnetic field penetration length and coherence length. Halperin, Lubensky and Ma established that in extreme type-1 superconductors the gauge field fluctuations make the superconducting phase transition first order.[77,78] In the opposite limit of extreme type-2 systems, Dasgupta and Halperin[79] demonstrated that the superconducting transition is second order in single-component systems and has the universality class of the inverted-3DXY model. The nature of the superconducting phase transition in this limit is the proliferation of vortex-loop excitations. The inverted-3DXY universality class can be demonstrated by duality mapping.[57,79–81]

The value of the Ginzburg-Landau parameter $\kappa = \lambda/\xi$ at which the phase transition changes from second to first order is difficult to establish. Early numerical works suggested that the tri-

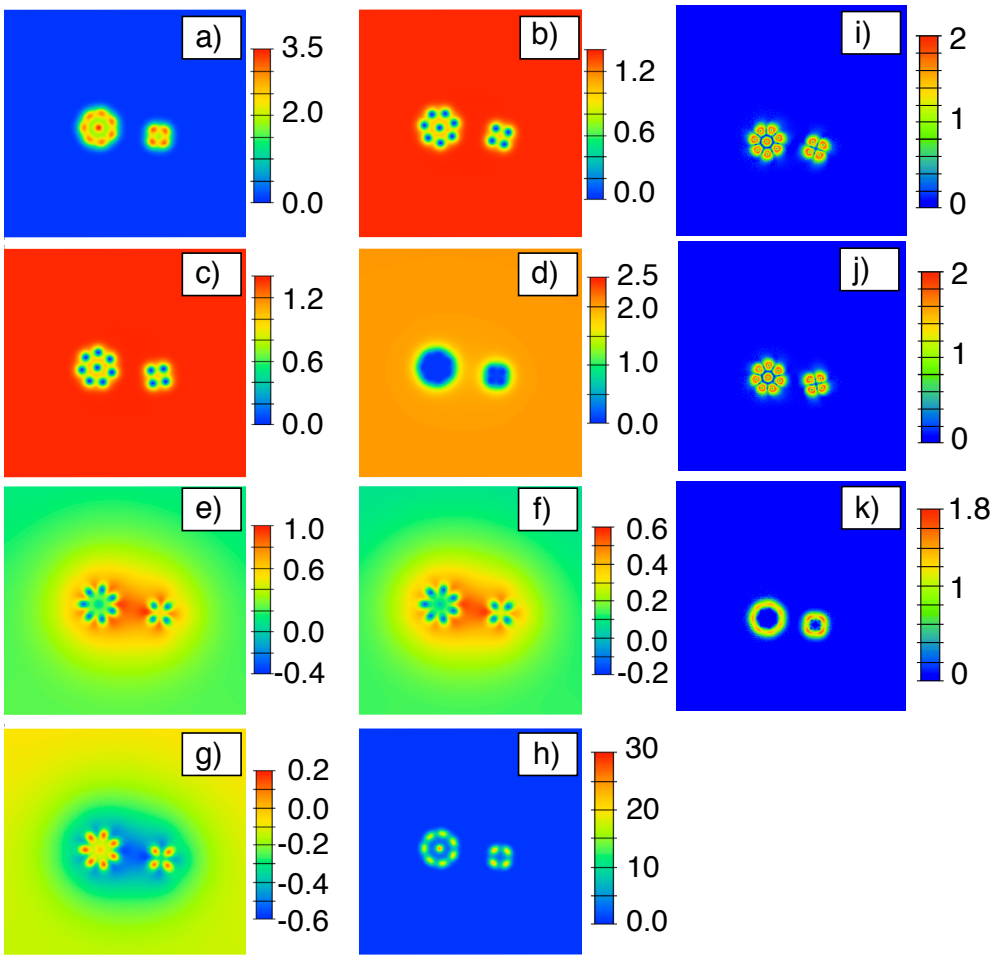

FIG. 9. Interacting vortex clusters with internally broken Z_2 symmetry in a frustrated three band superconductor. The snapshot represents a slowly evolving (quasi-stationary) state of the weakly interacting well-separated clusters. In this numerical computation, each of the clusters has with a good accuracy converged to a physical solution of GL equations, but the snapshot is taken during the slow evolution driven by the weak long-range intercluster interaction. The snapshot demonstrates the existence of long-range field variations associated with the soft mode. The soft mode, as discussed in the text, appears near the Z_2 phase transition. This produces weak but long-range intervortex forces. Displayed quantities are: a) Magnetic field, b-d) $|\psi_1|^2, |\psi_2|^2, |\psi_3|^2$, e) $|\psi_1||\psi_2|\sin\varphi_{12}$, f) $|\psi_1||\psi_3|\sin\varphi_{13}$), g) $|\psi_1||\psi_3|\sin\varphi_{23}$). The GL parameters are $\alpha_1 = -3,\ \beta_1 = 3,\ \alpha_2 = -3,\ \beta_2 = 3, \alpha_3 = 2,\ \beta_3 = 0.5, \eta_{12} = 2.25,\ \eta_{13} = -3.7$. The parameter set was chosen so that it lies in the regime where the ground state symmetry of the system without vortices is $U(1)$, but is close to the $U(1) \times Z_2$ region. Because of the disparity in vortex core size the effective interaction strengths $\tilde{\eta}_{ij}$ are depleted to different extents. As a consequence, a vortex cluster produces a bubble of state with broken $U(1) \times Z_2$ symmetry.

critical point does not coincide with the Bogomolnyi critical point.[82] The largest Monte Carlo simulations performed at this time[83,84] claim that the tricritical $\kappa_{\rm tri} = (0.76 \pm 0.04)$ is slightly

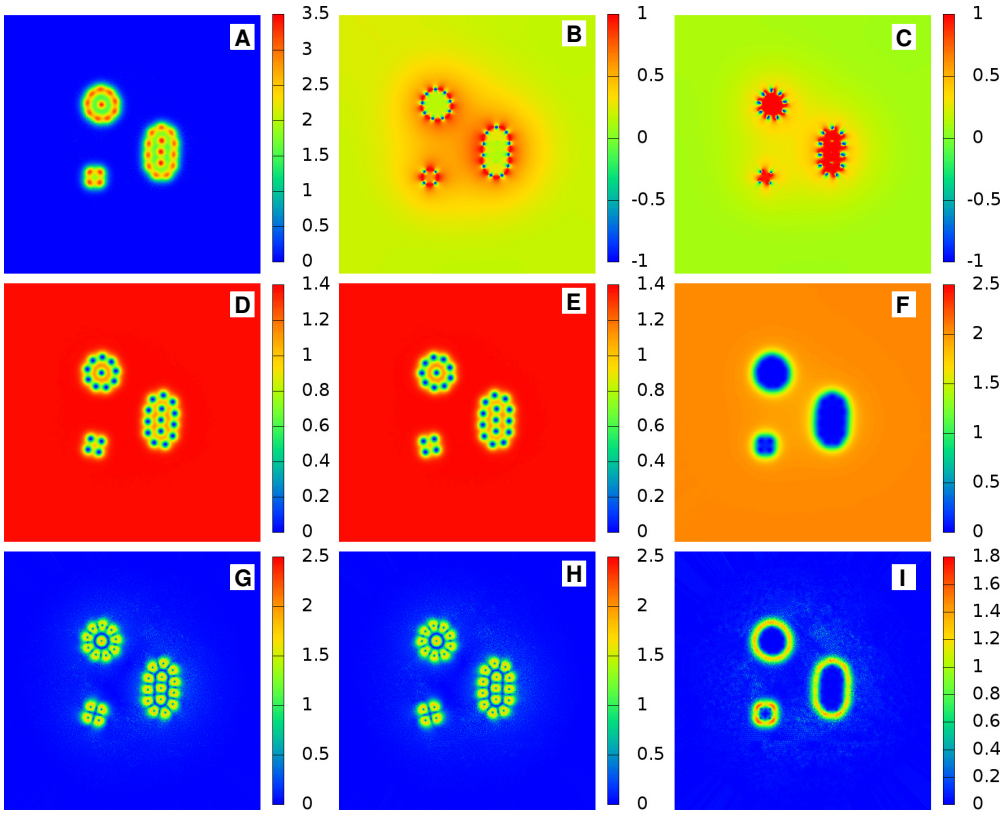

FIG. 10. Interacting vortex clusters with broken internal Z_2 symmetry in a frustrated three band superconductor. The panel **A** displays the magnetic field B. Panels **B** and **C** respectively display $\sin\varphi_{12}$ and $\sin\varphi_{13}$, the third phase difference can obviously be obtained from these two ones. Second line, shows the densities of the different condensates $|\psi_1|^2$ (**D**), $|\psi_2|^2$ (**E**), $|\psi_3|^2$ (**F**). The third line displays the supercurrent densities associated with each condensate $|J_1|$ (**G**), $|J_2|$ (**H**), $|J_3|$ (**I**). The parameter set here is the same as in Fig. 9.Here the difference compared to the previous picture, is that the sine of the phase differences is represented 'unweighted' by the densities in contrast to Fig. 9, clearly indicating that vortices create an area with broken Z_2 symmetry. Panel **C** now makes clear that the inner cluster is in a defined state $\varphi_{13} \approx \pi/2$ (whose opposite state would have been $-\pi/2$). Panel **B** gives a visualization of the long range interaction between the clusters.

smaller than the critical $\kappa_c = 1$, which, in our units, separates the type-1 regime with thermodynamically unstable vortices and the type-2 regime with thermodynamically stable vortices. In these works it is claimed that even in the weakly type-1 regime where the vortex interaction is purely attractive and vortices are not thermodynamically stable, the phase transition can be continuous. This raises the question about the nature of the phase transition in type-1.5 regime where by contrast vortices have long-range attractive interaction but are thermodynamically stable. The problem was investigated in the effective j-current model[85] where thermally excited vortices are

modeled by directed loops with long-range attractive, short-range repulsive interaction similar to the long-range interaction between vortices in GL model. The results indicate that the zero-field superconducting phase transition in type-1.5 materials can be first order.[85] This is in contrast to ordinary single-component GL theory which always has a continuous phase transition in the inverted 3d XY universality class in the parameter regime where vortices are thermodynamically stable. For the $s + is$ type-1.5 systems it was found that fluctuations can modify the mean-field phase diagrams quantitatively, resulting in reentrant phase transitions where Z_2 symmetry is broken by heating.[73]

X. CONCLUSION

We briefly outlined the basic concepts and gave a brief account on type-1.5 superconductivity that takes place in multicomponent systems. In general a superconducting state state is characterised by multiple coherence lengths ξ_i, $(i = 1, ..., M)$ arising from multiple broken symmetries or multiple bands. The type-1.5 state is the regime where some of the coherence lengths are larger and some smaller than the magnetic field penetration length: $\xi_1 \leq \xi_2 ... < \lambda < \xi_M \leq ... \leq \xi_N$ (here we absorbed the usual factor $1/\sqrt{2}$ into the definition of coherence lengths). Such a situation should rather generically arise in systems that have phase transitions between superconducting states that break different symmetries: at such phase transitions some of the coherence length diverge while other coherence lengths and magnetic field penetration length stay finite. Among various unconventional properties that the system acquires in this regime long-range attractive, short-range repulsive intervortex interaction potential. This allows a macroscopic phase separation into domains of Meissner and vortex states in an applied external field. This phase separation can also be accompanied by different broken symmetries in vortex clusters and Meissner domains. This regime leads to unconventional magnetic, thermal and transport properties.

XI. ACKNOWLEDGMENTS

We thank Julien Garaud for discussions and collaboration on this project. The work was supported by the Swedish Research Council Grant. No. 642-2013-7837 and Goran Gustafsson Foundation. J.C. was supported by Wenner-Gren foundation. The computations were performed on resources provided by the Swedish National Infrastructure for Computing (SNIC) at National

Supercomputer Center at Linköping, Sweden.

---

[1] E. Babaev and M. Speight, Phys. Rev. B **72**, 180502 (2005).

[2] L. Landau and V. Ginzburg, Zh. Eksp. Teor. Fiz **20**, 546 (1950).

[3] P. De Gennes, *Superconductivity of Metals and Alloys (Advanced Book Classics)* (Addison-Wesley Publ. Company Inc, 1999).

[4] A. A. Abrikosov, Sov. Phys.-JETP (Engl. Transl.);(United States) **5** (1957).

[5] L. Kramer, Phys. Rev. B **3**, 3821 (1971).

[6] E. Bogomol'nyi, Sov. J. Nucl. Phys. (Engl. Transl.); (United States) **24:4** (1976).

[7] J. Carlström, E. Babaev, and M. Speight, Phys. Rev. B **83**, 174509 (2011).

[8] V. Stanev and Z. Tešanović, Phys. Rev. B **81**, 134522 (2010).

[9] S. Maiti and A. V. Chubukov, Phys. Rev. B **87**, 144511 (2013).

[10] J. Carlström, J. Garaud, and E. Babaev, Phys. Rev. B **84**, 134518 (2011).

[11] E. Babaev, A. Sudbø, and N. Ashcroft, Nature **431**, 666 (2004).

[12] E. V. Herland, E. Babaev, and A. Sudbø, Physical Review B **82**, 134511 (2010).

[13] P. B. Jones, Monthly Notices of the Royal Astronomical Society **371**, 1327 (2006), http://mnras.oxfordjournals.org/content/371/3/1327.full.pdf+html.

[14] E. Babaev, Physical review letters **103**, 231101 (2009).

[15] H. Suhl, B. T. Matthias, and L. R. Walker, Phys. Rev. Lett. **3**, 552 (1959).

[16] A. J. Leggett, Progress of Theoretical Physics **36**, 901 (1966).

[17] D. Tilley, Proceedings of the Physical Society **84**, 573 (1964).

[18] M. Silaev and E. Babaev, Phys. Rev. B **85**, 134514 (2012).

[19] J. Garaud, D. F. Agterberg, and E. Babaev, Phys. Rev. B **86**, 060513 (2012).

[20] R. L. Frank and M. Lemm, Annales Henri Poincaré , 1 (2016).

[21] E. Babaev, J. Carlström, and M. Speight, Phys. Rev. Lett. **105**, 067003 (2010).

[22] M. Silaev and E. Babaev, Phys. Rev. B **84**, 094515 (2011).

[23] J. Carlström, J. Garaud, and E. Babaev, Phys. Rev. B **84**, 134515 (2011).

[24] V. Moshchalkov, M. Menghini, T. Nishio, Q. H. Chen, A. V. Silhanek, V. H. Dao, L. F. Chibotaru, N. D. Zhigadlo, and J. Karpinski, Phys. Rev. Lett. **102**, 117001 (2009).

[25] T. Nishio, V. H. Dao, Q. Chen, L. F. Chibotaru, K. Kadowaki, and V. V. Moshchalkov, Phys. Rev. B **81**, 020506 (2010).

[26] C. W. Hicks, J. R. Kirtley, T. M. Lippman, N. C. Koshnick, M. E. Huber, Y. Maeno, W. M. Yuhasz, M. B. Maple, and K. A. Moler, Phys. Rev. B **81**, 214501 (2010).

[27] S. J. Ray, A. S. Gibbs, S. J. Bending, P. J. Curran, E. Babaev, C. Baines, A. P. Mackenzie, and S. L. Lee, Phys. Rev. B **89**, 094504 (2014).

[28] I. Kawasaki, I. Watanabe, H. Amitsuka, K. Kunimori, H. Tanida, and Y. Ōnuki, Journal of the Physical Society of Japan **82**, 084713 (2013).

[29] T. Fujisawa, A. Yamaguchi, G. Motoyama, D. Kawakatsu, A. Sumiyama, T. Takeuchi, R. Settai, and Y. Ånuki, Japanese Journal of Applied Physics **54**, 048001 (2015).

[30] E. Dumont and A. C. Mota, Phys. Rev. B **65**, 144519 (2002).

[31] J. Garaud, E. Babaev, T. A. Bojesen, and A. Sudbø, arXiv preprint arXiv:1605.03946 (2016).

[32] J. Garaud and E. Babaev, Scientific reports **5** (2015).

[33] D. F. Agterberg, E. Babaev, and J. Garaud, Phys. Rev. B **90**, 064509 (2014).

[34] S. Parameswaran, S. Kivelson, E. Rezayi, S. Simon, S. Sondhi, and B. Spivak, Physical Review B **85**, 241307 (2012).

[35] M. G. Alford and G. Good, Physical Review B **78**, 024510 (2008).

[36] V. H. Dao, L. F. Chibotaru, T. Nishio, and V. V. Moshchalkov, Phys. Rev. B **83**, 020503 (2011).

[37] J. Gutierrez, B. Raes, A. Silhanek, L. Li, N. Zhigadlo, J. Karpinski, J. Tempere, and V. Moshchalkov, Physical Review B **85**, 094511 (2012).

[38] L. Li, T. Nishio, Z. Xu, and V. Moshchalkov, Physical Review B **83**, 224522 (2011).

[39] C. N. Varney, K. A. Sellin, Q.-Z. Wang, H. Fangohr, and E. Babaev, Journal of Physics: Condensed Matter **25**, 415702 (2013).

[40] J.-P. Wang, Phys. Rev. B **82**, 132505 (2010).

[41] J. A. Drocco, C. J. O. Reichhardt, C. Reichhardt, and A. R. Bishop, Journal of Physics: Condensed Matter **25**, 345703 (2013).

[42] Q. Meng, C. N. Varney, H. Fangohr, and E. Babaev, Physical Review B **90**, 020509 (2014).

[43] J. Garaud and E. Babaev, Phys. Rev. B **91**, 014510 (2015).

[44] A. Edström, Physica C: Superconductivity **487**, 19 (2013).

[45] P. Forgacs and Á. Lukács, arXiv preprint arXiv:1603.03291 (2016).

[46] A. Gurevich, Phys. Rev. B **67**, 184515 (2003), cond-mat/0212129.

[47] A. Gurevich, Physica C: Superconductivity **456**, 160 (2007).

[48] M. E. Zhitomirsky and V.-H. Dao, Phys. Rev. B **69**, 054508 (2004).

[49] J. Garaud, M. Silaev, and E. Babaev, ArXiv e-prints (2016), arXiv:1601.02227 [cond-mat.supr-con].

[50] E. Babaev, Phys. Rev. Lett. **89**, 067001 (2002).

[51] J. M. Speight, Phys. Rev. D **55**, 3830 (1997), hep-th/9603155.

[52] N. S. Manton and P. Sutcliffe, *Topological solitons* (Cambridge University Press, 2004) cambridge, UK: Univ. Pr. (2004) 493 p.

[53] J. Pearl, Appl. Phys. Lett. **5**, 65 (1964).

[54] E. Bogomol'nyi and A. Vainshtein, Sov. J. Nucl. Phys.(Engl. Transl.);(United States) **23** (1976).

[55] D. Saint-James, G. Sarma, and E. J. Thomas, *TYPE-II SUPERCONDUCTIVITY.*, Tech. Rep. (CEN, Saclay, France, 1969).

[56] M. Shifman, *Advanced Topics in Quantum Field Theory: A Lecture Course* (Cambridge University Press, 2012).

[57] B. V. Svistunov, E. S. Babaev, and N. V. Prokof'ev, *Superfluid states of matter* (Crc Press, 2015).

[58] A. Jacobs, J. Low Temp. Phys. **10**, 137 (1973).

[59] M. C. Leung and A. E. Jacobs, J. Low Temp. Phys. **11**, 395 (1973).

[60] G. Eilenberger and H. Büttner, Zeitschrift fur Physik **224**, 335 (1969).

[61] A. E. Jacobs, Phys. Rev. B **4**, 3029 (1971).

[62] Y. N. Ovchinnikov, Journal of Experimental and Theoretical Physics **88**, 398 (1999).

[63] Y. N. Ovchinnikov, Journal of Experimental and Theoretical Physics **117**, 480 (2013).

[64] Q. Meng, C. N. Varney, H. Fangohr, and E. Babaev, ArXiv e-prints (2016), arXiv:1605.00524 [cond-mat.supr-con].

[65] R. Diaz-Mendez, F. Mezzacapo, W. Lechner, F. Cinti, E. Babaev, and G. Pupillo, Physical Review Letters **118**, 067001 (2017).

[66] E. Smørgrav, J. Smiseth, E. Babaev, and A. Sudbø, Physical Review Letters **94**, 96401 (2005).

[67] T. K. Ng and N. Nagaosa, Europhysics Letters **87**, 17003 (2009).

[68] S.-Z. Lin and X. Hu, Phys. Rev. Lett. **108**, 177005 (2012).

[69] J. Garaud, J. Carlström, and E. Babaev, Phys. Rev. Lett. **107**, 197001 (2011).

[70] J. Garaud, J. Carlström, E. Babaev, and M. Speight, Phys. Rev. B **87**, 014507 (2013).

[71] J. Garaud and E. Babaev, Phys. Rev. Lett. **112**, 017003 (2014).

[72] D. Weston and E. Babaev, Phys. Rev. B **88**, 214507 (2013).

[73] J. Carlström and E. Babaev, Phys. Rev. B **91**, 140504 (2015).

[74] M. Silaev and E. Babaev, Phys. Rev. B **88**, 220504 (2013).

[75] M. Silaev, J. Garaud, and E. Babaev, Phys. Rev. B **92**, 174510 (2015).

[76] J. Garaud, M. Silaev, and E. Babaev, Physical Review Letters **116**, 097002 (2016), arXiv:1507.04712 [cond-mat.supr-con].

[77] B. I. Halperin, T. C. Lubensky, and S.-K. Ma, Phys. Rev. Lett. **32**, 292 (1974).

[78] S. Coleman and E. Weinberg, Phys. Rev. D **7**, 1888 (1973).

[79] C. Dasgupta and B. I. Halperin, Phys. Rev. Lett. **47**, 1556 (1981).

[80] M. E. Peskin, Annals of Physics **113**, 122 (1978).

[81] P. R. Thomas and M. Stone, Nuclear Physics B **144**, 513 (1978).

[82] J. Bartholomew, Phys. Rev. B **28**, 5378 (1983).

[83] S. Mo, J. Hove, and A. Sudbø, Phys. Rev. B **65**, 104501 (2002).

[84] J. Hove, S. Mo, and A. Sudbø, Phys. Rev. B **66**, 064524 (2002).

[85] H. Meier, E. Babaev, and M. Wallin, Physical Review B **91**, 094508 (2015).